

**LIQUID-LIQUID EXTRACTION FROM SINGLE
DROPS AT ELEVATED TEMPERATURES**

By

Charles Kennady Huff

Bachelor of Science

Texas Technological College

Lubbock, Texas

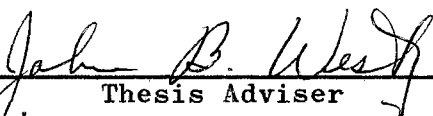
1961

**Submitted to the faculty of the Graduate School of the
Oklahoma State University in partial fulfillment
of the requirements of the degree of
MASTER OF SCIENCE
May, 1963**

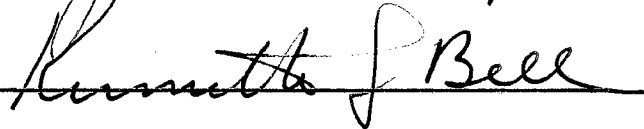
JAN 7 1964

LIQUID-LIQUID EXTRACTION FROM SINGLE
DROPS AT ELEVATED TEMPERATURES

Thesis Approved:



Thesis Adviser





Dean of the Graduate School

541989

PREFACE

The importance of liquid-liquid extraction increases with the increase of separation problems in modern chemical industries. With the exception of extended surface units, most types of extraction equipment operate by dispersing one phase as droplets in the second liquid phase. In order to properly design liquid-liquid extraction equipment, knowledge of the extraction mechanism is desirable, along with an understanding of drop behavior.

The effect of temperature on the extraction process was investigated. Attempts were made to correlate mass transfer rates in terms of the various chemical and physical properties of the system.

I am indebted to many for their guidance and suggestions throughout the course of the investigation. Drs. J. B. West, R. N. Maddox, and K. J. Bell, were particularly helpful in the literature search and procurement of materials needed. Mr. E. E. McCroskey offered many suggestions and gave much aid during the construction of the apparatus. I would also like to express my gratitude to my fellow graduate students, who gave suggestions and encouragement when they were needed the most. I am indebted to Phillips Petroleum Company for personal financial assistance during the past year.

TABLE OF CONTENTS

Chapter	Page
I. INTRODUCTION.	1
II. LITERATURE SURVEY OF SINGLE DROPLET EXTRACTION. . .	4
Description of the Droplets with No Mass	
Transfer	4
End Effects.	6
Free Rise.	9
III. EXPERIMENTAL APPARATUS AND PROCEDURE.	16
Experimental Apparatus	16
Experimental Procedure	21
IV. RESULTS AND DISCUSSION.	24
Experimental Results	24
Evaluation of Results.	25
V. CONCLUSIONS AND RECOMMENDATIONS	47
Conclusions.	47
Recommendations.	48
A SELECTED BIBLIOGRAPHY	50
APPENDIX	
A DEFINITION OF TERMS.	53
B PHASE EQUILIBRIUM DATA	55
C PHYSICAL PROPERTIES OF THE EQUILIBRATED PHASES . . .	70
D EXPERIMENTAL DATA AND CALCULATIONS	79

LIST OF TABLES

Table	Page
I. Effect of Temperature on Free Rise Transfer Efficiency.	30
II. Effect of Temperature on the Correlation Factor, R	35
III. Equilibrium and Phase Boundary Data for the 95 Per Cent Aq. Phenol--Cetane--O-Xylene System at 130 ^o F.	58
IV. Equilibrium and Phase Boundary Data for the 95 Per Cent Aq. Phenol--Cetane--O-Xylene System at 145 ^o F.	61
V. Equilibrium and Phase Boundary Data for the 95 Per Cent Aq. Phenol--Cetane--O-Xylene System at 160 ^o F.	64
VI. Equilibrium and Phase Boundary Data for the 95 Per Cent Aq. Phenol--Cetane--O-Xylene System at 175 ^o F.	67
VII. Refractive Index--Composition Data for the Cetane--O-Xylene System	73
VIII. Densities of the Equilibrated Phases.	75
IX. Viscosities of the Equilibrated Phases.	76
X. Interfacial Tensions Between the Equilibrated Phases.	77
XI. Diffusivities of the Equilibrated Phases.	78
XII. Transfer of Phenol to Cetane Drops.	84
XIII. Transfer of O-Xylene to Cetane Drops.	85
XIV. Transfer of O-Xylene from Cetane Drops.	86

XV.	Calculated Concentrations of Each Stage of Extraction.	87
XVI.	Calculated Dimensionless Groups	88
XVII.	Calculated Dimensionless Groups for Use in Lileeva and Smirnov's Correlation	89

LIST OF ILLUSTRATIONS

Figure	Page
1. Schematic Diagram of Extraction Apparatus.	17
2. Experimental Nozzles	20
3. Effect of Free Rise Time on Transfer Efficiency for the System Phenol--Cetane.	27
4. Effect of Temperature on End Effect Transfer Efficiencies	28
5. Effect of Temperature on Free Rise Transfer Efficiency for the System Phenol + Xylene-- Cetane	31
6. Effect of Temperature on Free Rise Transfer Efficiency for the System Phenol--Cetane	32
7. Effect of Temperature on Free Rise Transfer Efficiency for the System Phenol--Cetane + Xylene	33
8. Effect of Temperature on the Correlation Factor, R, for the System Phenol--Cetane	36
9. Effect of Temperature on the Correlation Factor, R, for the System Phenol + Xylene--Cetane	37
10. Effect of Temperature on the Correlation Factor, R, for the System Phenol--Cetane + Xylene	38
11. Dimensionless Correlation for the System Phenol-- Cetane + Xylene.	41
12. Dimensionless Correlation for the Systems Phenol-- Cetane and Phenol + Xylene--Cetane	42
13. Dimensionless Correlation Proposed by Thorsen and Terjesen	44
14. Dimensionless Correlation Using Exponents Suggested by Lileeva and Smirnov	46

15.	Ternary Diagram for the 95 Per Cent Aqueous Phenol-- Cetane--O-Xylene system at 130 ^o F.	59
16.	Distribution Data of O-Xylene Between Cetane and 95% Aqueous Phenol at 130 ^o F	60
17.	Ternary Diagram for the 95 Per Cent Aqueous Phenol--Cetane--O-Xylene System at 145 ^o F.	62
18.	Distribution Data of O-Xylene Between Cetane and 95% Aqueous Phenol at 145 ^o F	63
19.	Ternary Diagram for the 95 Per Cent Aqueous Phenol-- Cetane--O-Xylene System at 160 ^o F.	65
20.	Distribution Data of O-Xylene Between Cetane and 95% Aqueous Phenol at 160 ^o F	66
21.	Ternary Diagram for the 95 Per Cent Aqueous Phenol-- Cetane--O-Xylene System at 175 ^o F	68
22.	Distribution Data of O-Xylene Between Cetane and 95% Aqueous Phenol at 175 ^o F	69
23.	Refractive Index--Composition Curve for the Cetane-- O-Xylene System	74
24.	Effect of Free Rise Time on Transfer Efficiency for the System Phenol + Xylene--Cetane.	82
25.	Effect of Free Rise Time on Transfer Efficiency for the Phenol--Cetane + Xylene System.	83
 Plate		
I.	Extraction Column	18

CHAPTER I

INTRODUCTION

In recent years the unit operation of liquid-liquid extraction has assumed an increasing importance as the separation problems of modern process chemistry have become more complex. Extraction is a potentially useful method of separating components of solutions which are particularly difficult or expensive to separate by the conventional methods of distillation, absorption, evaporation, or chemical precipitation. Extraction can be used when the substance or substances to be recovered are relatively nonvolatile, close-boiling, heat-sensitive, or present in relatively small amounts.

With the exception of extended surface units and packed towers, which operate by the film-contact mechanism, nearly all types of liquid-liquid extraction equipment used today secure contact through the dispersion of one phase as droplets. It is thus apparent that a study of the motion of liquid drops and mass transfer to and from the drops in a second liquid medium should provide basic information for the design of most liquid-liquid extractors.

Some investigators (14, 24, 20, 30) have studied the effect of drop size and drop motion on stage efficiency and capacity of the equipment. Others have conducted investigations to determine the rate of mass transfer to and from droplets (10, 17, 4, 32, 23, 9, 25).

Licht and Conway (23) found that the capacity of a spray column is dependent upon the rates of flow of both the continuous and the dispersed phases, upon which phase is dispersed, upon the direction of extraction, and in certain cases upon the inlet solute concentration. They also found that three separate stages of extraction occur in the life of each drop. It would be difficult to design a spray tower without knowledge of the extraction in each stage.

Other investigators found that circulation sometimes occurred within the droplet and this circulation had a great effect upon the mass transfer (10, 11, 20, 8, 3). West (36) and Johnson (17) suggested mechanism of mass transfer for stagnant drops. Handlos and Baron (10), Kronig and Brink (21), Garner (7), and others (11), (22) have proposed various mechanisms for mass transfer from droplets at various stages of circulation.

Garner (7) felt that extraction rates could be correlated with the various chemical and physical properties of the system with better results than the various suggested mechanisms.

Statement of Problem

The objectives of this extraction study to be attained were:

1. To determine the effect of temperature on rates of mass transfer from single drops.
2. To correlate the mass transfer rate constants in terms of physical and chemical properties.

These objectives were accomplished by transferring o-xylene, 1-methylnaphalene, and mesitylene to and from cetane droplets

dispersed in phenol. This was done at temperatures of 175°F, 160°F, 145°F, and 130°F.

CHAPTER II

LITERATURE SURVEY OF SINGLE DROPLET EXTRACTION

The investigation of liquid-liquid extraction from single droplets can be placed in two main groups, those that studied drop characteristics in the absence of mass transfer, and those that studied the mass transfer. The latter can also be classified into two main groups, those which studied end effects, and those that investigated mass transfer during free rise.

Description of the Droplets With No Mass Transfer

Several workers have investigated the differences in behavior of liquid drops compared to rigid spheres falling or rising through a liquid medium (14, 24, 20). Sherwood, Evans, and Longcor (32) were among the first investigators to notice the differences in the shape of small and large droplets. They found that the smaller drops appeared to be spherical, but the larger drops were noticeably flat, with horizontal axes sometimes twice the vertical axes. Hu and Kintner (14) thought that the main reasons for the difference between the motion of liquid drops and that of rigid spheres are the deformation and oscillation of the drops as well as the flow on the drop surface and the circulation inside the drops. They found that when no mass transfer takes place, liquid drops behave the same as a rigid sphere up to Reynolds numbers of about 300. Above this

value, the drag coefficient, C_D , starts to increase rather abruptly within a narrow Reynolds number range.

Licht and Narasimhamurty (24) found that the interfacial tension is a very important factor controlling the rate of rise or fall of liquid droplets. They found that the lower the interfacial tension, the greater the deviation from solid spheres. They also found that the larger the drops the greater the deviation.

Hu and Kintner (14) experimented with drop diameters. They developed an equation for the critical drop diameter, d_c , above which the drop ruptures.

$$d_c = \left[1.452 \times 10^{-2} \left(\frac{\sigma_i}{\Delta \rho} \right) \right]^{1/2} \quad (1)$$

Klee and Treybal (20) found that internal drop circulation could increase the rate of rise or fall over that observed for rigid spheres. They also found that drop eccentricity, which is inversely proportional to interfacial tension, has a greater influence on drop velocities, and in the reverse direction, than has internal circulation. Drop eccentricity is simply the ratio of the largest horizontal diameter to the largest vertical diameter.

Elzinga and Banchemo (5) found that after the drops form and break away from the tip, there is a short period in which they accelerate to their terminal velocity. From motion picture studies they found that the drops always had reached at least 95% of terminal velocity after traveling 2 inches. It was also found that when surface-active material is present, causing oscillations, the drop velocity is less than with no oscillations. The natural frequency of oscillation for a drop can be estimated with a relation developed

for liquid spheres. The primary mode of this oscillation is given by the following equation.

$$F = \left[\frac{192 \sigma}{(3e_d + 2e)d^3} \right]^{1/2} \quad (2)$$

As can be seen, the natural frequency of a liquid drop decreases as its size increases.

Strom and Kintner (33) investigated wall effects for single drops. They said that the reduction of drop velocity is caused by a reduction in the area available for fluid to flow around the drop. They found the ratio of terminal velocity in a cylinder to terminal velocity in an infinite field to be

$$\frac{v}{v_\infty} = \left[1 - \left(\frac{d}{D} \right)^2 \right]^{1.43} \quad (3)$$

Where:

d = drop diameter

D = cylinder diameter

Because of the large difference in mass transfer rates in rigid and liquid spheres, the behavior of the drop is important to mass transfer studies. Before trying to analyze mass transfer mechanisms, the investigator should study the behavior of the drops.

End Effects

Among the first investigators reporting end effects in liquid-liquid extraction were Johnson and Bliss (16), Sherwood, Evans, and Longcor (32), and West, et al. (36).

Sherwood, Evans, and Longcor (32) determined the end effect by

plotting the logarithm of the fraction of unextracted solute against column height. The resulting straight line was extrapolated to zero column height to give an end effect of approximately 40% of the total material transferred. West, et al. (36), used the same procedure and found with a similar plot an end effect of about 20%. Some investigators discount the experimental results of West because of the use of tygon tubing, which contaminated the system. Both of these investigators assumed that the total end effect was due to drop formation. Licht and Pansing (25) found that mass transfer in drop formation was small compared to the mass transfer in coalescence

Johnson, Hamielec, Ward, and Golding (18) used a unique apparatus for studying end effects. They dropped the drops through the continuous phase but had a Linseed oil separating phase between the continuous phase and the coalesced dispersed phase. They found that the formation end effect may include several transfer mechanisms--transfer inside or at the nozzle and excessive transfer rates during the unsteady period usually occurring after drop release. The end effect at the exit end is due to coalescence, and may include transfer to the settled dispersed phase. Normally for experiments at constant drop size and formation rate the end effects are independent of column height.

Johnson and Hamielec (17) define the transfer efficiencies for the various stages as follows:

$$\text{Formation efficiency, } E_{f1} = \frac{C_1 - C_2}{C_1 - C_*} \quad (4)$$

$$\text{Efficiency of the steady fall period, } E_m = \frac{C_2 - C_3}{C_2 - C_*} \quad (5)$$

$$\text{Coalescence efficiency, } E_{f2} = \frac{C_3 - C_4}{C_3 - C_*} \quad (6)$$

$$\text{Total efficiency, } E_T = \frac{C_1 - C_4}{C_1 - C_*} \quad (7)$$

Here C_1 , C_2 , C_3 , and C_4 are the uniformly mixed concentrations at the beginning and end of each stage, and C_* is the concentration which would be in equilibrium with the other phase.

Heertjes (12) developed an equation for the formation efficiency by assuming transient diffusion into the surface of the drop as it is formed.

$$E_{f1} = \frac{20.6}{d} \sqrt{\frac{D \Theta_f}{\pi}} \quad (8)$$

Where:

d = drop diameter

D = molecular diffusivity

Θ_f = drop formation time

By use of Higbie's (13) penetration theory, Johnson and Hamielec (9) derived an expression for the mass transfer efficiency during coalescence.

$$E_{f2} = \frac{2A_i}{v} \sqrt{\frac{D \Theta}{\pi}} \quad (9)$$

Where:

A_i = interfacial area at coalescence

v = drop volume

Johnson and Hamielec also combined their equation for coalescence

with the formation equation of Heertjes to obtain an equation for the transfer efficiency of the combined end effects

$$E_F = E_{f_1} + E_{f_2} - E_{f_1} \times E_{f_2} \quad (10)$$

$$E_F = \left(\frac{20.6}{d} + \frac{2A_i}{v} \right) \sqrt{\frac{D \Theta}{\pi}} - \left(\frac{41.2 A_i D \Theta}{dv \pi} \right) \quad (11)$$

Licht and Pansing (25) found that in general a plot of the logarithm fraction solute unextracted versus drop fall time is not a straight line all the way back to zero fall time. Therefore, extraction during drop formation cannot be determined by extrapolation. They also found that extraction during drop coalescence is proportional to drop concentration and diameter.

Free Rise

Probably more work has been done on trying to find a suitable mechanism for mass transfer during free rise than on any other stage of single droplet extraction. Sherwood, Evans, and Longcor (32) tried to use Newman's (29) equation for unsteady-state diffusion in a stagnant sphere, but without success. It thus became apparent that the amount of transfer depends upon the amount of internal circulation within the droplet.

Several investigators have postulated different patterns of circulation within the drop. McDowell and Myers (29) found that if the viscosity of the liquid in the drop is low enough compared with the viscosity of the continuous-phase fluid, the liquid in the drop will circulate. For negligible interfacial tension and for a drop Reynolds number less than unity, Kronig and Brink (21)

derived an equation for diffusion into a circulating drop with no continuous phase resistance:

$$E_m = 1 - \frac{3}{8} \sum_{n=1}^{\infty} B_n^2 e^{-\left[\lambda_n \frac{16D\Theta}{r^2} \right]} \quad (12)$$

Where:

B = Coefficient

λ = Eigenvalue

D = Molecular diffusivity

r = Drop radius

Θ = Contact time of drop for steady rise period

Elzinga and Banchemo (5) obtained the same equation for the case of a finite continuous-phase resistance.

Handlos and Baron (10) proposed a circulation model which included radial motion. They also proposed an equation for mass transfer efficiency using their circulation model:

$$E_m = 1 - 2 \sum_{n=1}^{\infty} B_n e^{-\frac{\lambda_n D \Theta Pe'}{2048d^2}} \quad (13)$$

Where:

Pe' = Modified Peclet number, $(Vd)/D(1 + u_i/u_o)$.

They claim that only one term of this series with $\lambda = 2.88$ need be used. They also derived an effective diffusivity as a function of the radius:

$$E(r) = \frac{D Pe'}{2048} \times (6r^2 - 8r + 3) \quad (14)$$

Korchinski (2) proposed a correlation factor, R, for diffusion inside drops which he used in a modified Vermeulen (35) equation:

$$E_m = 1 - e^{-\left[\frac{RD \pi^2 \Theta}{r^2} \right]} \quad (15)$$

Where R has a value of 2.25. Korchinski showed his equation to represent the Kronig and Brink model well.

Johnson and Hamielec (17) have developed equations for both high and low extraction efficiencies. They are modifications of the Korchinski equation.

For low efficiency:

$$E_m = 0.905 \sqrt{\frac{RD \pi^2 \Theta}{r^2}} + 0.0189 \quad (16)$$

They combined this equation with their equation for end effects to give an equation for the total transfer efficiency.

$$E_T = 0.905(1 - E_F) \sqrt{\frac{RD \pi^2 \Theta}{r^2}} + (0.0189 + 0.981 E_F) \quad (17)$$

At low efficiencies and for a constant R, a plot of E_T against the square root of contact time should yield a straight line, the intercept of which may be used to find E_F . Knowing E_F , one can use the slope of the line to obtain the correlation factor R.

At higher E_m values all but the first term of the Korchinski equation are negligible.

$$\ln(1 - E_m) = -\lambda_1^2 \frac{RD \Theta}{r^2} + \ln 6B \quad (18)$$

Combining with end effects

$$\ln(1 - E_T) = -\lambda_1^2 \frac{RD \Theta}{r^2} + \ln 6B(1 - E_F) \quad (19)$$

For high-efficiency data and a constant R , one should plot $\ln(1 - E_T)$ against time of contact to obtain E_F from the intercept and R from the slope.

For noncirculating drops R should be 1. For a circulating drop under the Kronig and Brink model, R should be about 3. Johnson and Hamielec used the Handlos and Baron model for comparison purposes and found the correlation factor, R , is directly proportional to the modified Peclet number.

$$R = \frac{Pe'}{2048} \quad (20)$$

Many investigators found that it was very difficult to find a mechanism for mass transfer which their data would fit. They instead tried to correlate the mass transfer in terms of various physical and chemical properties of the system.

Handlos and Baron (10) proposed that

$$Sh = Sh(Re, Sc, We, \frac{e'}{e}, \frac{u'}{u}, \frac{D'}{D}, m) \quad (21)$$

They did not, however, try to solve for the complete equation.

Lileeva and Smirnov (26) studied the equations of motion, continuity, and diffusion with the proper initial and boundary conditions to determine the important variables.

$$Ki = Ki(Re_c, Re_d, Ar, Fo, Pr_c, Pr_d, m, \Gamma, \phi) \quad (22)$$

Where:

Ki = Kirpichev diffusion number, $\frac{Kd}{D}$

$$Ar = \frac{d^3}{u_c^2} \frac{e_c}{g} (e_c - e_d)$$

Fo = Fourier diffusion no., $\frac{\Theta D}{d^2}$

Pr = Prandtl diffusion no.

m = Distribution coefficient

$\Gamma = \frac{\bar{d} + d}{\bar{d}}$ \bar{d} = diameter of apparatus

ϕ = Phase volume ratio, $\frac{V_c}{V_d}$

They found that the experimental data gave two equations:

$$Ki = 3.79 \times 10^{-9} Re_{rel}^{.5} Ar^2 Fo^{.42} \phi^{-.7} m^{-.5} Pr_d^{.5} Pr_c^{.5} \Gamma^{-1.5} \quad (23)$$

and

$$Ki = 2.44 \times 10^{-12} Re_d^{.9} Re_c^{.2} Ar^{1.8} Fo^{-.14} M^{-.5} Pr_d^{.5} Pr_c^{.5} \Gamma^{-1.5} \quad (24)$$

Baird and Hamielec (1), using boundary layer theory, derived the following equation:

$$Sh = \left[\frac{2}{\pi} Pe \int_0^{\pi} U^* \sin^2 \Theta d\Theta \right]^{1/2} \quad (25)$$

Where:

Θ = Angle relative to front stagnation point

$U^* = \frac{u^*}{u^o}$ u^* is the surface velocity
 u^o is the velocity relative to continuous phase

U^* is found by the equation:

$$U^* = \frac{10 + 2A}{8 + 3X} \sin \Theta + f(B_1) \sin \Theta \cos \Theta \quad (26)$$

Where:

A, B are functions of Re and X

X = Ratio of viscosities

Akselrud, as cited by Garner (7), used boundary layer theory to solve Fick's law for diffusion from a solid sphere into a fluid stream flowing past it. His equation was

$$Sh = 0.8Re^{0.5}Sc^{.33} \quad (27)$$

Garner, Foord, and Tayeban (7) found from boundary layer theory that the Schmidt number exponent ranged from 1/3 with no internal circulation to 1/2 for full circulation. They found that the Reynolds number had an exponent of 1/2 for spherical drops but that the exponent would change for deformed drops. Realizing that the full mechanism is very complex, they suggested an equation of the form $Sh = a + bRe^{0.5}Sc^m$ as a first approximation. They found that their data best fitted the line

$$Sh = -126 + 1.8Re^{0.5}Sc^{0.42} \quad (28)$$

Garner suggested that the difference in mass transfer between solid and liquid spheres was due to internal circulation.

Hurst (15) found that the correlation was helped by the inclusion of the Weber number. His correlation was

$$Sh = -610 + .46Re^{0.5}Sc^{0.47}We^{0.9} \quad (29)$$

Thorsen and Terjesen (34) felt that though internal circulation might have some effect on mass transfer rates, "the large difference in mass transfer between liquid and solid drops could not be accounted for in this manner." They felt that the toroidal vortex, which is caused by the separation of the boundary layer, was the cause of the large differences. Turbulence on the back

surface of the sphere is caused by this vortex and increases mass transfer by physical mixing. This boundary layer separation with the formation of a toroidal vortex behind the sphere takes place at Reynolds numbers about 17. With increasing Reynolds numbers the vortex gains strength as the separation point moves forward.

They found that the exponent on the Schmidt number is always 1/3, and they correlated their data by the equation

$$\text{Sh} = - 178 + 3.62\text{Re}^{0.5}\text{Sc}^{0.33} \quad (30)$$

CHAPTER III

EXPERIMENTAL APPARATUS AND PROCEDURE

Experimental Apparatus

The column used in this study was an all-glass, jacketed column. The dispersed phase flowed in from the bottom and rose through the continuous phase. The continuous phase entered at the top. The experimental apparatus is shown in Figure 1 and in Plate I.

Column Construction

The studies of droplet extraction were performed in an all-glass, jacketed column which was three inches I.D. and twenty-six inches high. Hot oil was pumped from a constant-temperature bath through the jacket to keep the column at a constant temperature. The constant-temperature bath was heated with a coil heater and was controlled to within 0.5°F with a Fisher-Serfass electronic relay and a Fisher mercury probe.

The lines carrying the continuous phase were all made of 1/4 inch stainless steel tubing. The valves on these lines were 1/4 inch Hoke stainless steel needle valves with teflon gaskets. The continuous phase flow rate was measured with a Fischer and Porter rotometer. The lines carrying the dispersed phase were made of 1/4 inch copper tubing. The valves and fittings were made of brass. The lines were connected to the glass capillary

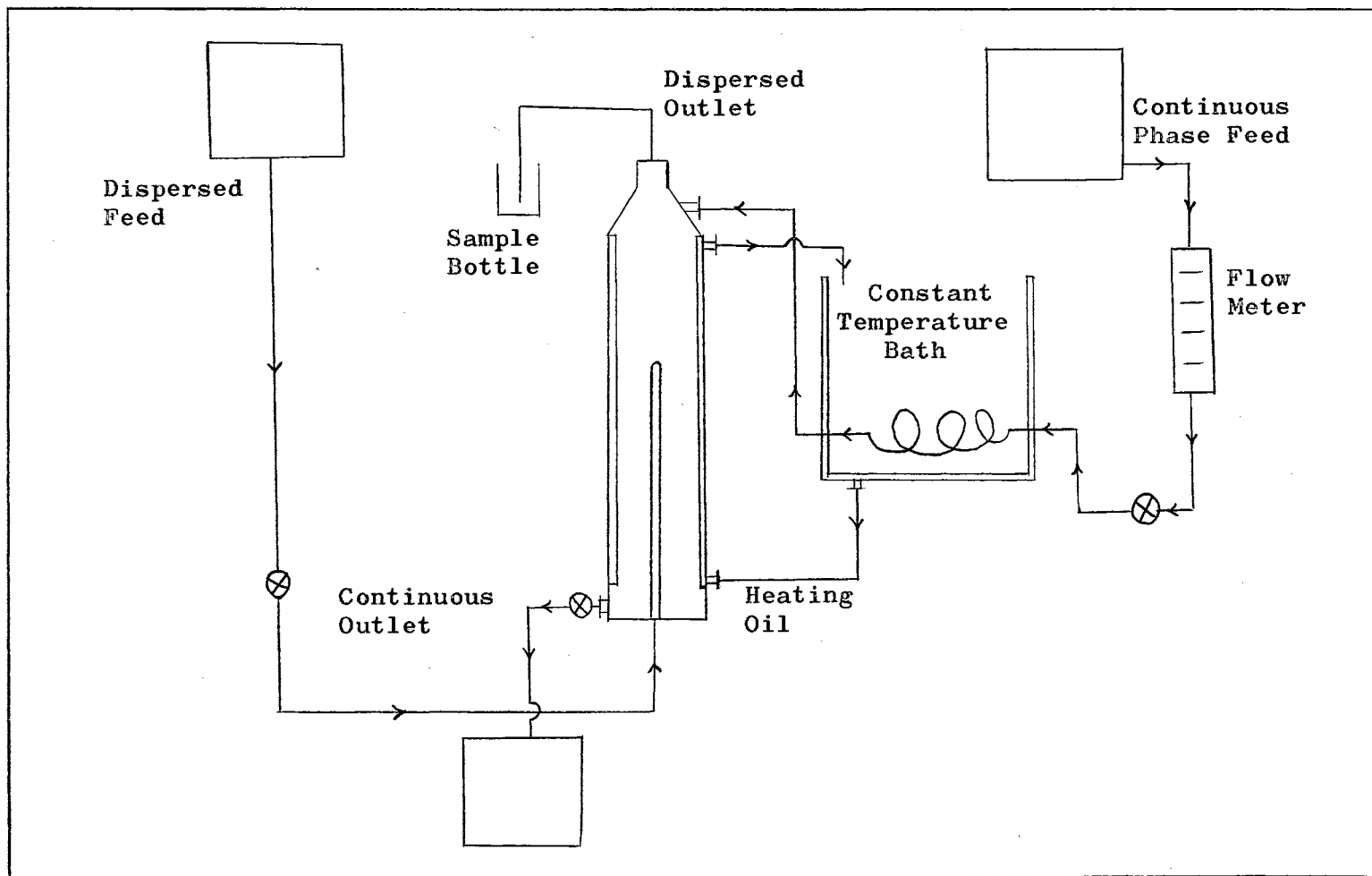
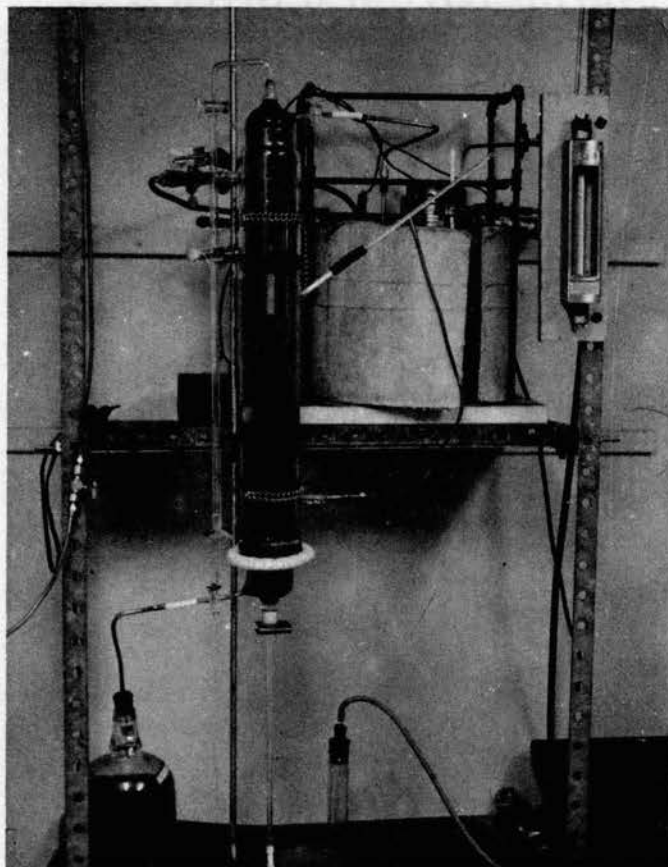


Figure 1, Schematic Diagram of Extraction Apparatus

PLATE I

EXTRACTION COLUMN



inlets and outlets by 1/4 inch I.D. teflon tubing. The teflon tubing was heated in boiling water and then slipped over the glass capillaries and stainless steel tubing, resulting in a sealed fitting.

The nozzles for the dispersed phase were mounted upon a three-foot piece of 2 mm I.D. glass capillary tubing. The capillary tubing was inserted into a teflon stopper in the bottom of the column. The glass tubing could be slipped up and down to change the height of the nozzle. This was the method used to change the effective height of the column. The glass capillary was connected to the dispersed phase feed line with teflon tubing, over which tygon tubing was slipped to make it leak-proof. The nozzles were connected to the glass tubing by teflon tubing.

Nozzles

The two nozzles used in this study were made from hypodermic needle bases, from which the needles had been pulled. The needle bases were silver soldered to a three inch piece of 1/4 inch stainless steel tubing. The first nozzle, which was just the needle hole, gave small drops from which the extraction approached 100 per cent. The second nozzle was beveled from the inside, which allowed the drops to grow as they moved up toward the end. Figure 2 shows the construction of the two nozzles

Several other nozzles were tried, but they all allowed the continuous phase to run down into the dispersed feed line. The unsatisfactory ones were made of 2 mm glass capillary, 1 mm glass capillary, 2 mm stainless steel capillary, and 2 mm copper capillary.

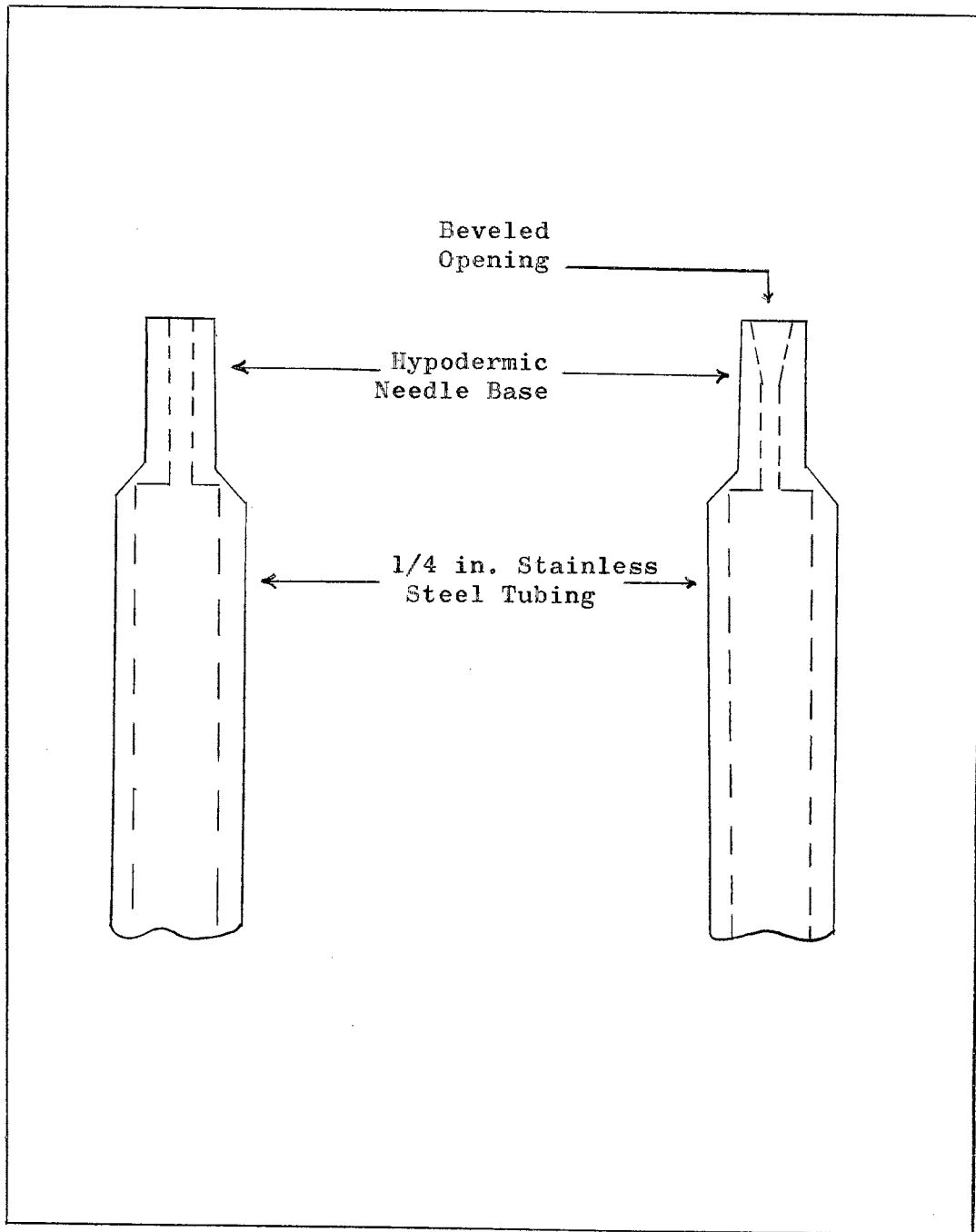


Figure 2, Experimental Nozzles

The dispersed phase was collected in a cylinder 5/8 inch in diameter which was built onto the top of the column. The coalescence area remained constant in spite of small changes in the height of the interface. This type of collecting device is favored over a funnel, where the area, and thus the end effects, will change with small changes in the height of the interface.

Materials

A solution of 95% phenol--5% water was used as the continuous phase. The phenol was U.S.P. fused crystals and was dissolved in deionized water to give the correct solution. Practical grade cetane was the main component of the dispersed phase. The three different solutes used were highest purity o-xylene, highest purity mesitylene, and practical grade 1-methylnaphthalene. All the chemicals were purchased from Matheson, Coleman, and Bell.

Experimental Procedure

Column Operation

At the start of each run the heater and the circulating pump were started to bring the column up to temperature. This usually took about two hours. The column was then filled with the continuous phase and allowed to heat for another hour. During a run the continuous phase feed was heated by flowing through a coil which was in the constant temperature bath. The temperature was observed from a thermometer which was in a thermal well about half way up the column. When the continuous phase was at the desired temperature, the run was started.

The dispersed phase was forced out of the nozzle by a slight

positive air pressure on the feed tank. The dispersed phase then rose through the continuous phase and was collected at the top of the column. The dispersed phase flow was measured by the counting of droplets, and was controlled by a needle valve. The free rise time was measured to the nearest 0.1 second with a stop watch.

The height of the interface was controlled by adjusting the outlet flow of the continuous phase. The continuous phase inlet flow was set at the first of each run by the inlet needle valve.

A sample was taken by allowing the interface to rise, forcing the collected dispersed phase over into a weighing bottle. Each sample was approximately 7 milliliters.

Analysis

The samples were allowed to cool and then were weighed on a Mettler Automatic balance to the nearest 0.01 milligrams. The sample was then poured into a micro separatory funnel. Ten milliliters of 20% NaOH solution was then added and the mixture was shaken for five minutes. The weighing bottle was washed with another 10 milliliters of the NaOH solution, which was added to the separatory funnel. This was done to assure that all the oil had been transferred to the separatory funnel and all the phenol had been converted to sodium phenolate. The oil was then transferred to another weighing bottle and weighed. The difference of the weights of the two solutions was the weight of the phenol in the sample.

A drop of the oil was then placed on the slide of a Spencer 1591 refractometer, and the refractive index of the oil solution was read. The composition of the oil was then calculated from a

refractive index--composition curve. In this way the chemical composition of a sample was found. By knowing the concentration of the dispersed feed, the amount of solute transfer was calculated.

Chapter IV

RESULTS AND DISCUSSION

Experimental Results

Drop Characteristics

The effect of temperature on mass transfer rates was determined for two droplet sizes and five systems. The five systems were pure cetane--phenol, cetane + o-xylene--phenol, cetane--xylene + phenol, cetane + 1-methylnaphthalene--phenol, and cetane + mesitylene--phenol. The two droplet sizes were 0.135 and 0.203 cm in diameter. Only qualitative studies were done with the 0.135 cm drops and with the 1-methylnaphthalene and mesitylene systems. It was discovered that extraction from the smaller droplets approached total extraction. In both the 1-methylnaphthalene and mesitylene systems the extraction efficiencies were less than with the xylene. This would seem to indicate that the larger the solute molecule the slower the mass transfer rates, as would be expected.

All the drops were spherical, or nearly so. The drops showed very little oscillation in rise path at the two low temperatures, but oscillations in path could be observed visually at the higher temperatures. The drops of the cetane + xylene--phenol system rose in a very random path at 175^oF, which would indicate interfacial turbulence. With this same system at

the smaller drop size it was observed that the droplets ascended in a zig-zag path for about eight inches, and then rose from there in a straight line. It was assumed that as the concentration difference at the drop--continuous phase interface was reduced, the interfacial turbulence became negligible.

Data Reproducibility

Three samples were taken during each run. The compositions of the three samples reproduced within 1% on all runs with the exception of the runs made with pure cetane--phenol systems. The top of the column was not jacketed, causing a temperature gradient within the sampling tube. Phenol would precipitate from the sample, causing random composition readings. Also, the phenol--cetane samples were analyzed by weight, and the other systems were analyzed by refractive index.

Evaluation of Results

End Effects

Transfer efficiencies were calculated from the equation

$$E_T = \frac{C_1 - C_4}{C_1 - C^*} \quad (7)$$

for each column height. Johnson, et al (18), stated that a plot of $\ln(1 - E_T)$ versus free-rise time will have an intercept of $\ln(1 - E_F)$, provided there is negligible continuous phase resistance. Therefore, $\ln(1 - E_T)$ was plotted against free-rise time and extrapolated to zero free-rise time. The intercept of this plot was $\ln(1 - E_T)$ for the combined end effects. Since the smallest value of the free-rise time was around one second, it

was felt that the extrapolation could be made without serious error. Figure 3 is a typical example of a $\ln(1 - E_T)$ versus free rise time plot. The plot for the other systems are included in Appendix D.

Only the total end effect efficiencies were calculated, since only one coalescence area was used. The experimental end effect efficiencies plotted against the temperature gave a straight line for the temperature range studied, as can be seen in Figure 4. The theoretical end effects were calculated using Johnson and Hamielec's (17) combined end effects equation, but the results were very unsatisfactory. Their equation gave efficiencies which were too high, sometimes over 100%.

Transfer Efficiencies for Free Rise

The transfer efficiencies for free rise were calculated by the equation

$$E_m = \frac{C_2 - C_3}{C_2 - C^*} \quad (5)$$

Since only the total end effects were known, C_2 was a hypothetical concentration at the start of free rise assuming no extraction during coalescence and C_3 was the concentration at the end of each run. C_2 was calculated by subtracting the amount of solute extracted by total end effects from the total solute of the feed.

The transfer efficiencies for free rise were calculated from the experimental data and compared with the various mechanisms suggested by other investigators. The Handlos and Baron (10) model, which has no term for molecular diffusion, gave transfer efficiencies which were up to 50% higher than the experimental

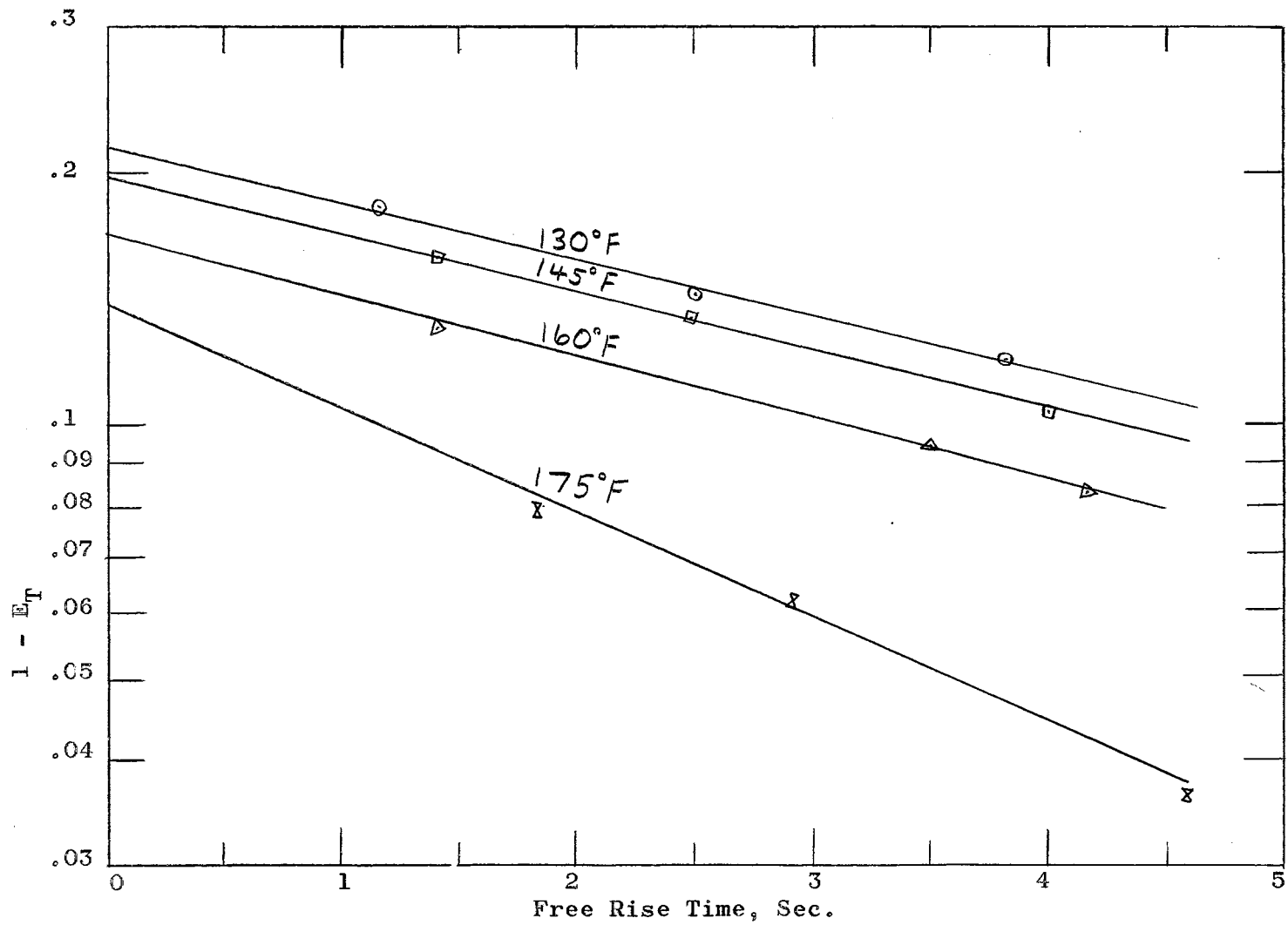


Figure 3, Effect of Free Rise Time on Transfer Efficiency for the System Phenol--Cetane

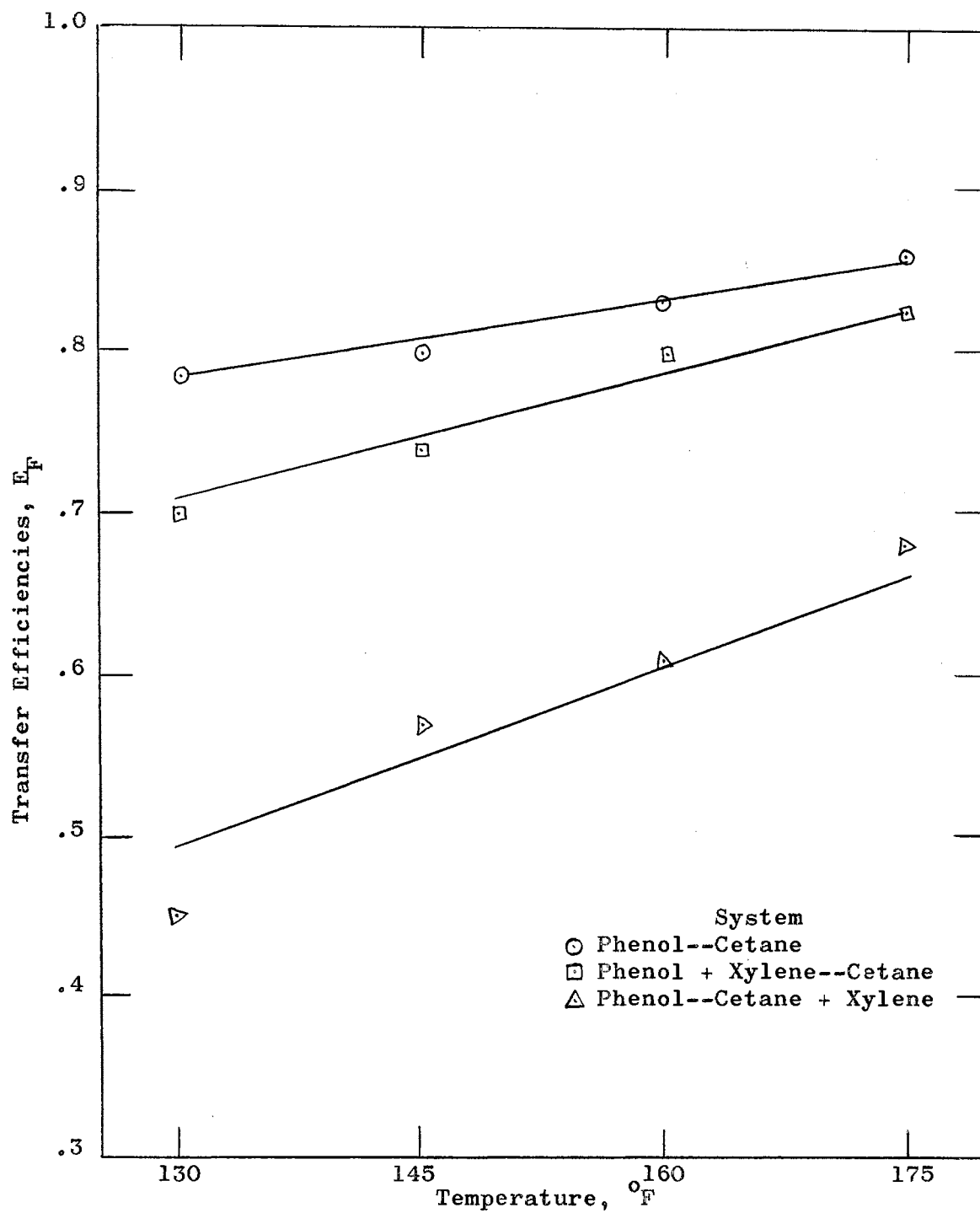


Figure 4, Effect of Temperature on End Effect Transfer Efficiencies

ones. The efficiencies calculated by this model decreased with increasing temperature. The experimental efficiencies increased with increasing temperature, as did the Kronig and Brink (21) model. The Kronig and Brink model gave transfer efficiencies which were always lower than the experimental values. They varied from 13.5% low at low temperatures to 35% low at higher temperatures. The Handlos and Baron equation is considered to predict the upper limit to transfer rates, while the Kronig and Brink equation approaches the lower limit. Table I and Figures 5, 6, and 7 show the effect of temperature on free-rise transfer efficiency. The point at 175°F in the cetane--phenol system was suspected to be bad when the data was taken because it could not be reproduced.

Correlation Factor, R

Calderbank and Korchinski (2) suggested that a multiplication factor of molecular diffusivity could be used to compare transfer rates in circulating systems to transfer rates encountered in stagnant drops. According to the Handlos and Baron model, the multiplication factor of the molecular diffusivity is directly proportional to the modified Peclet number.

$$R = \frac{Pe'}{2048} = \frac{V d}{D(1 - \frac{u_d}{u_c})2048} \quad (31)$$

The multiplication factor was calculated from the above equation. R was also determined empirically from the data by use of the total Handlos and Baron equation and by use of Johnson's model.

TABLE I
EFFECT OF TEMPERATURE ON FREE-RISE
TRANSFER EFFICIENCY

<u>Temperature</u>	<u>Experimental</u>	<u>Kronig and Brink Model</u>
System: Phenol--Cetane		
130	0.388	0.345
145	0.478	0.373
160	0.510	0.415
175	0.740	0.447
System: Phenol + Xylene--Cetane		
130	0.446	0.385
145	0.481	0.415
160	0.563	0.461
175	0.575	0.522
System: Phenol--Cetane + Xylene		
130	0.545	0.437
145	0.560	0.472
160	0.845	0.505
175	0.869	0.561

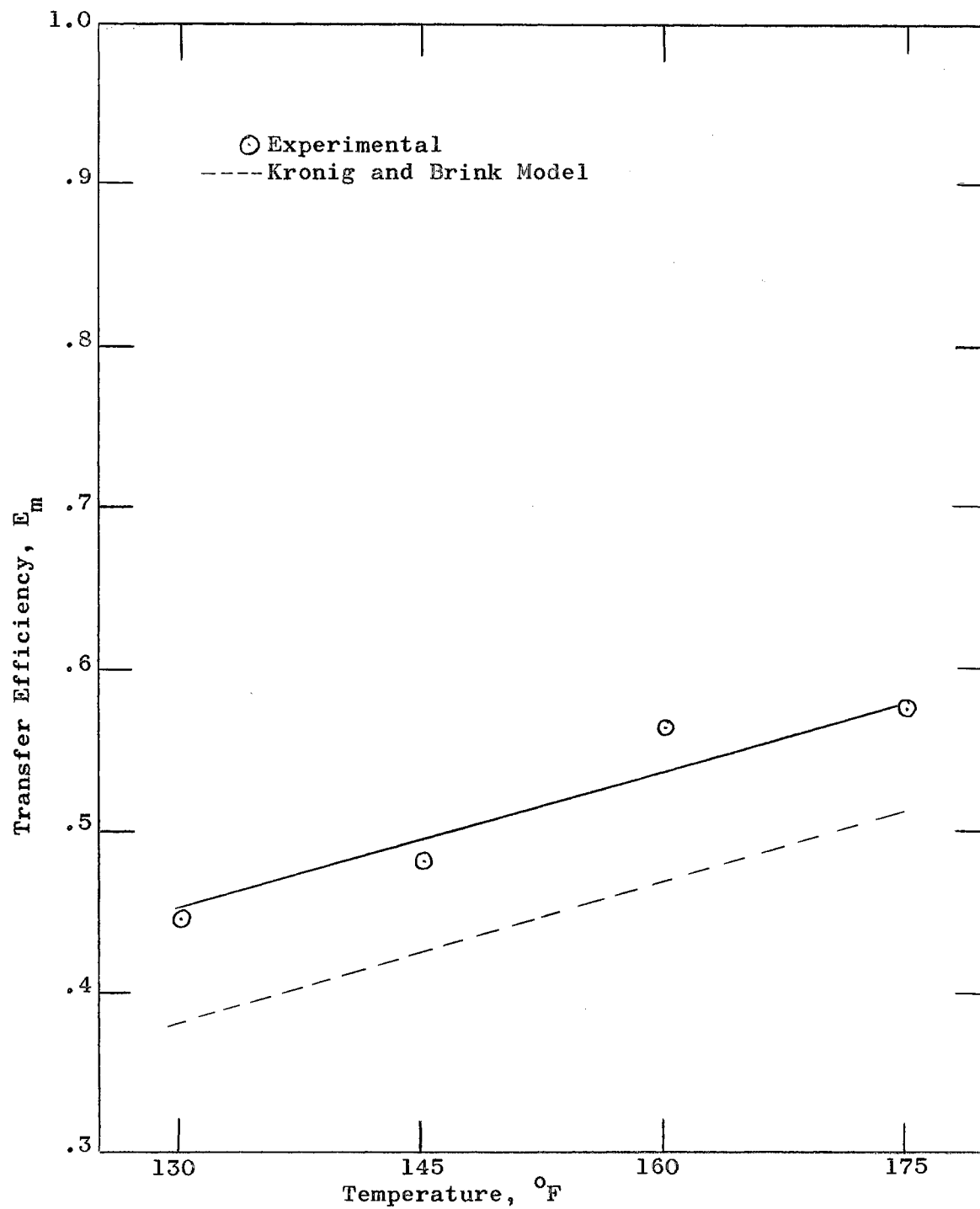


Figure 5, Effect of Temperature on Free Rise Transfer Efficiency for the System Phenol + Xylene--Cetane

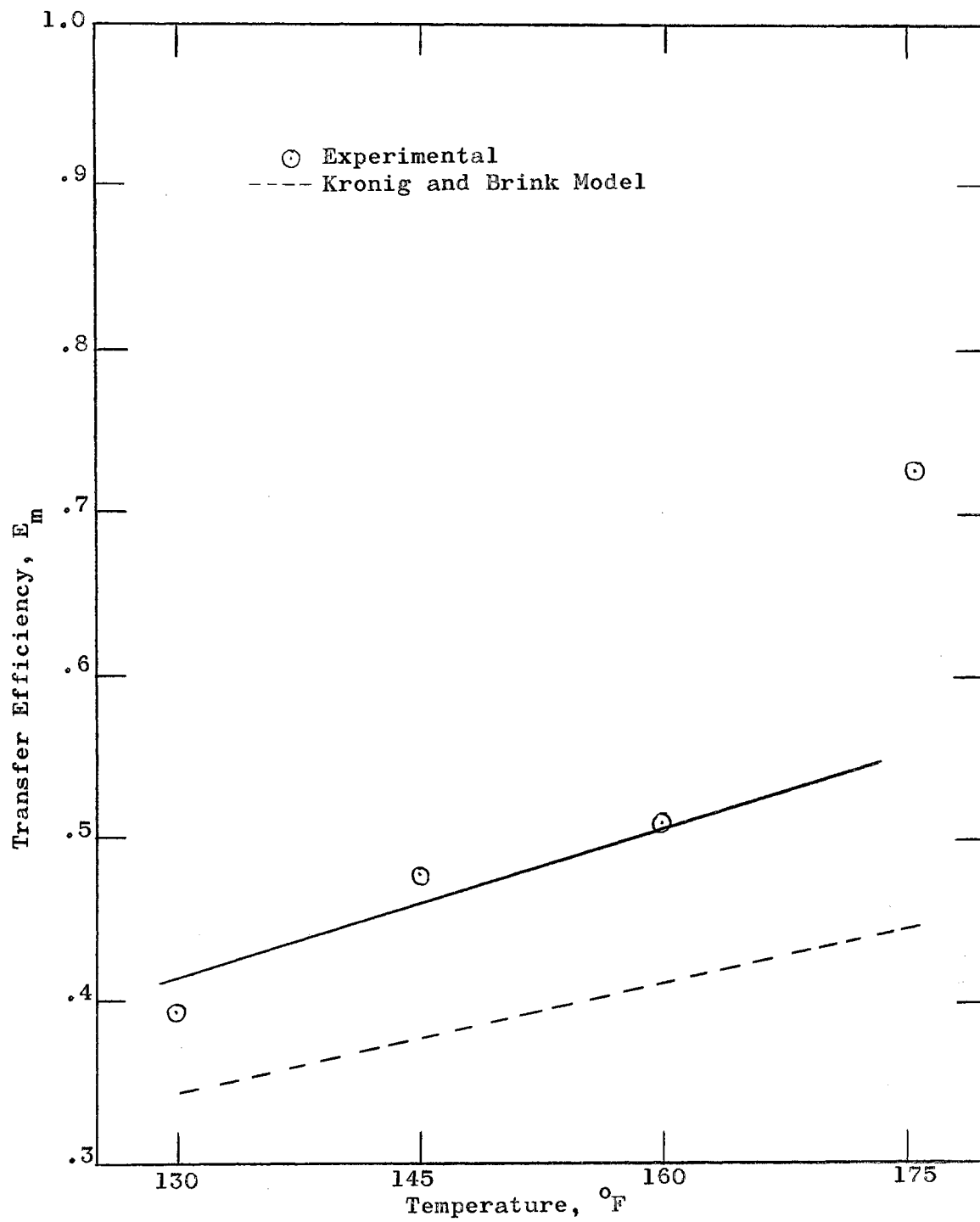


Figure 6, Effect of Temperature on Free Rise Transfer Efficiency for the System Phenol--Cetane

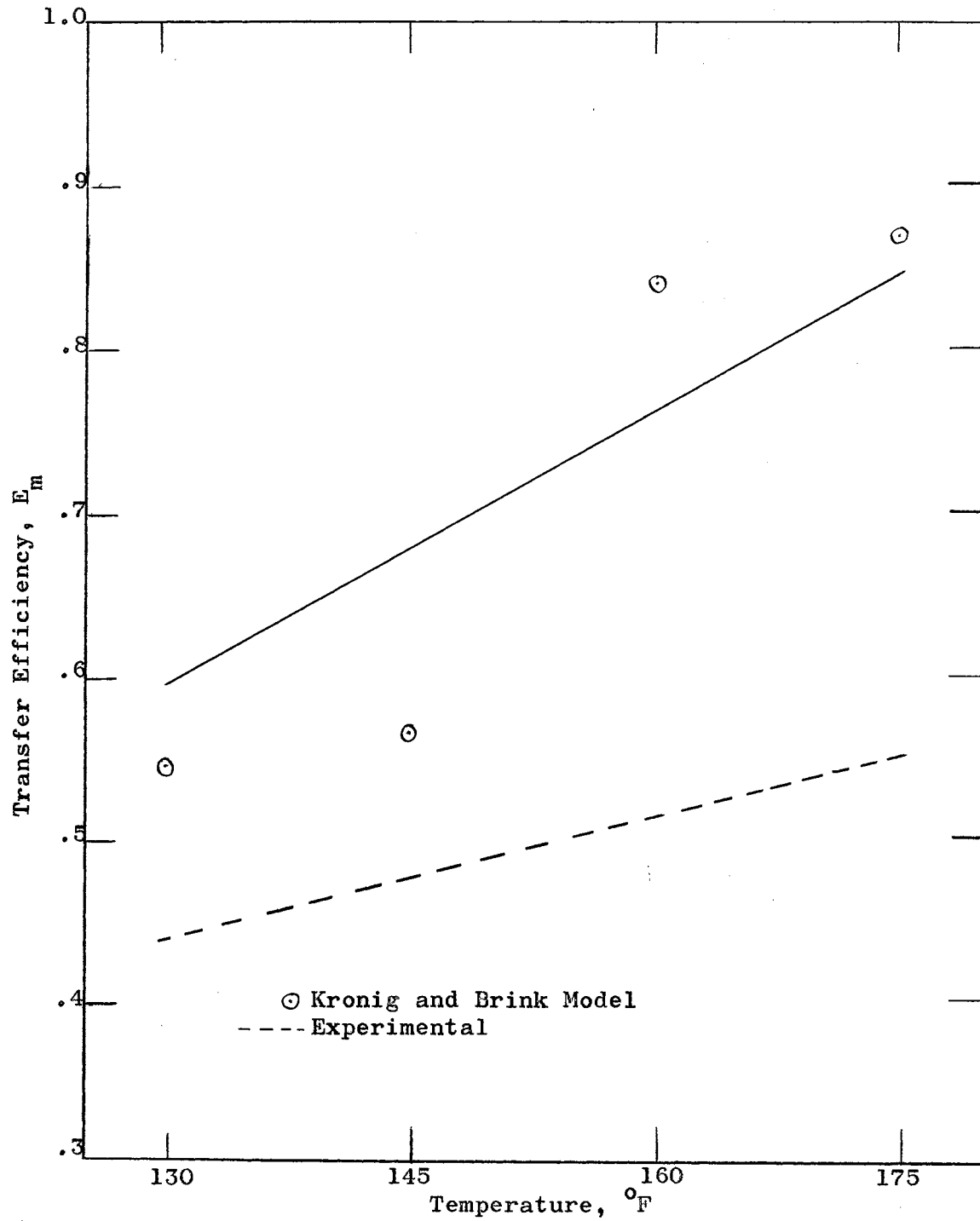


Figure 7, Effect of Temperature on Free Rise Transfer Efficiency for the System Phenol--Cetane + Xylene

Handlos and Baron:

$$\ln(1 - E_m) = \ln(2B^2) - \frac{16D\Theta R}{d^2} \quad (32)$$

Johnson:

$$\ln(1 - E_m) = -\frac{\lambda RD\Theta}{d^2} \quad (33)$$

To obtain R from Johnson's equation, one should plot $\ln(1 - E_m)$ against time of contact and calculate R from the slope.

Both the experimental calculations gave higher values of R than those calculated from equation (31), with the Handlos and Baron equation giving the highest. As Table II and Figures 8, 9, and 10 show, the value of R decreases with increasing temperature for all three calculations. The Handlos and Baron experimental values varied from the calculated by as much as 140%, while the Johnson experimental values varied from the calculated by as much as 60%.

Calderbank and Korchinski suggested that the correlation factor was directly related to the Reynolds number. Several investigators (12, 7, 18, 28) found that the correlation factor increased with increasing Reynolds number. Also, they found that the drops began to oscillate at correlation factors of about 20. However, in both this work and in Kim's (19) study, the values of R were higher than those found by others for similar Reynolds number. This would indicate that R is a function of more than just the Reynolds number. Also, in this study and in Kim's, the Reynolds number increased with temperature, while R decreased.

TABLE II
EFFECT OF TEMPERATURE ON THE
CORRELATION FACTOR, R

<u>Temperature</u>	<u>Calculated</u>	<u>Experimental</u>		
		<u>Handlos</u>	<u>and Baron</u>	<u>Johnson</u>
System: Phenol--Cetane				
130	34.0	58.0		48.0
145	27.1	53.6		39.8
160	20.5	45.0		31.8
175	16.5	43.0		29.3
System: Phenol + Xylene--Cetane				
130	31.1	56.0		42.5
145	25.8	46.0		36.0
160	19.6	42.4		27.8
175	13.0	30.0		18.8
System: Phenol--Cetane + Xylene				
130	18.5	42.3		32.5
145	15.1	36.6		27.4
160	12.6	35.0		23.0
175	10.3	33.0		18.0

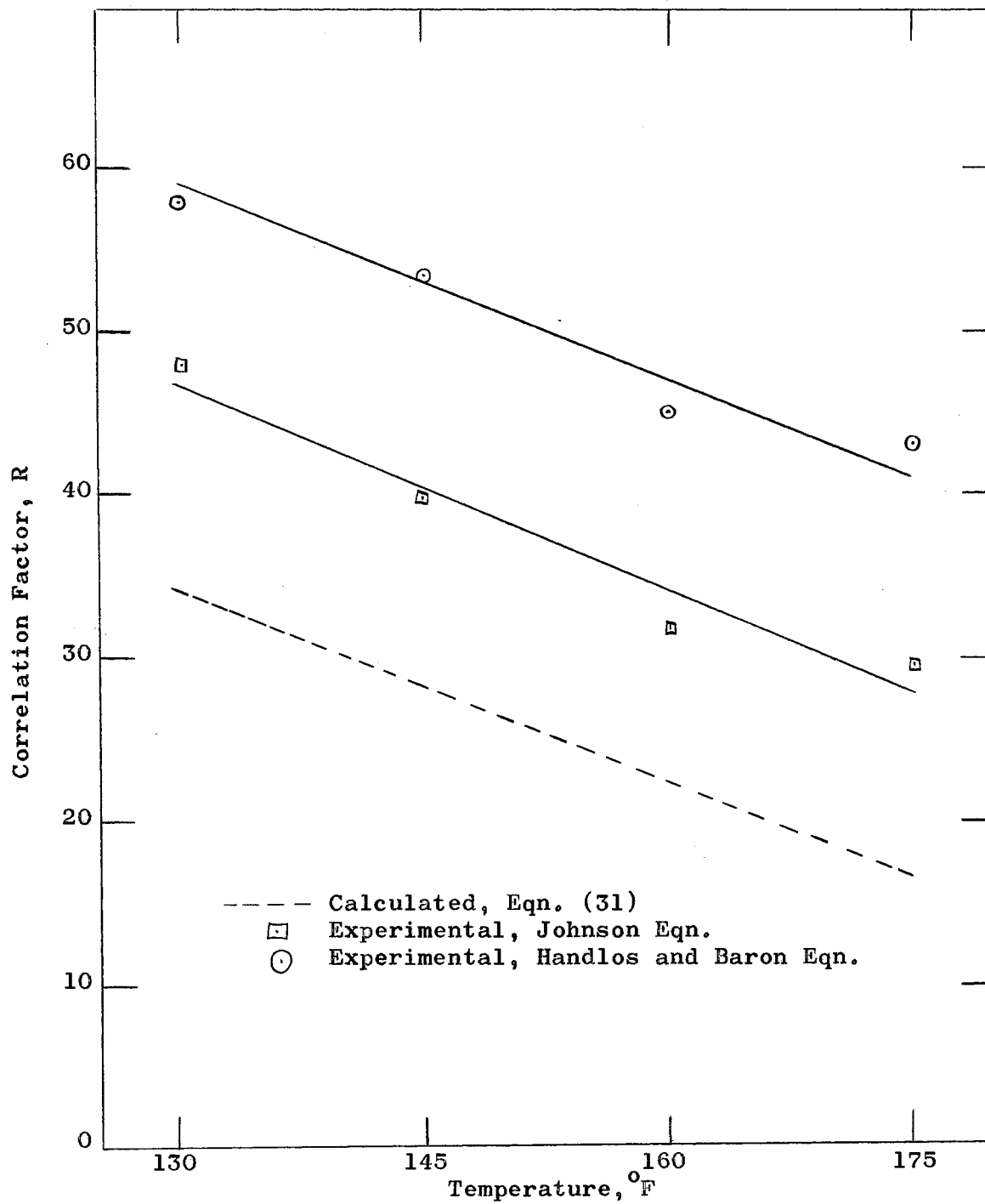


Figure 8, Effect of Temperature on the Correlation Factor, R, for the System Phenol--Cetane

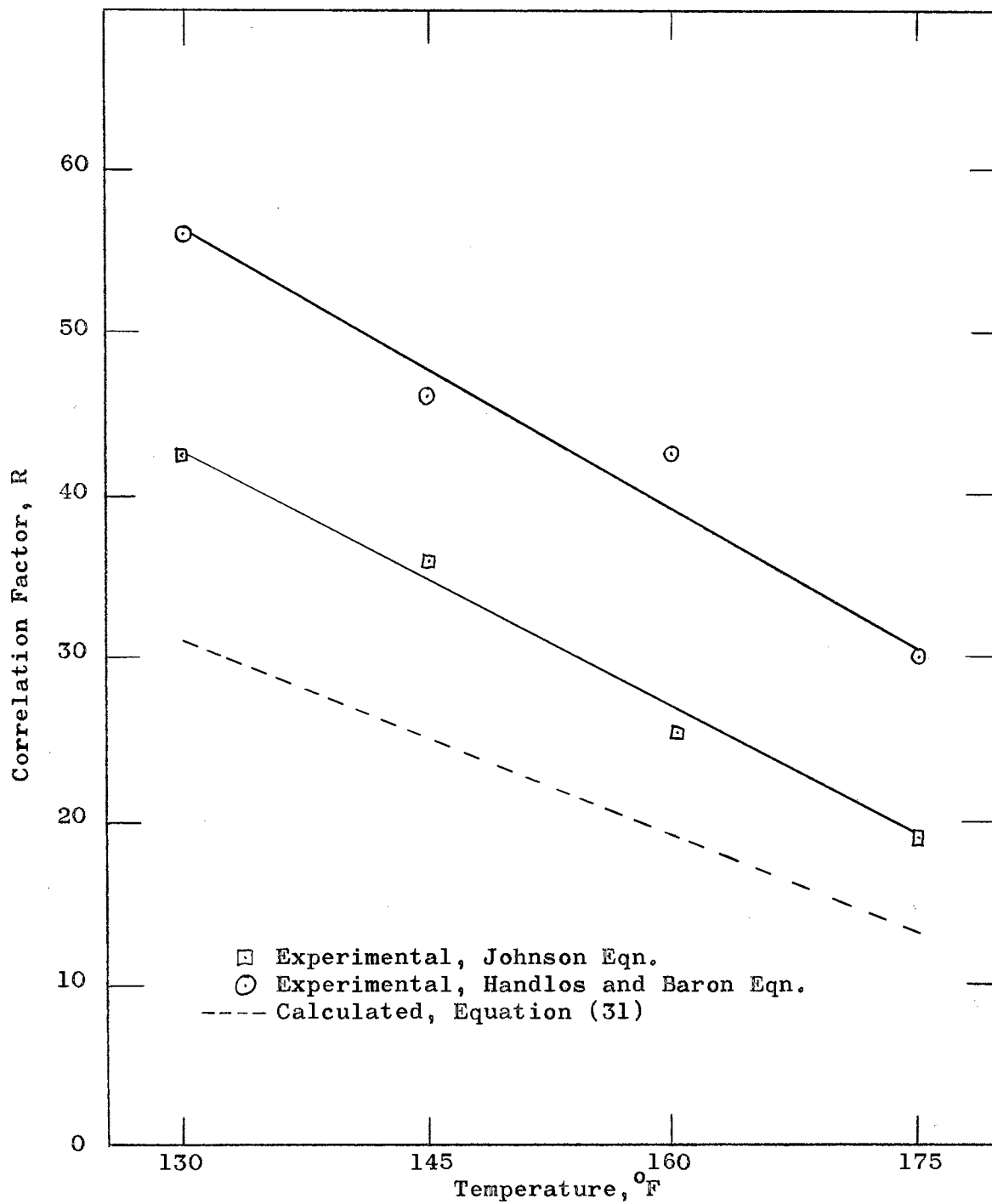


Figure 9, Effect of Temperature on the Correlation Factor, R, for the System Phenol + Xylene--Cetane

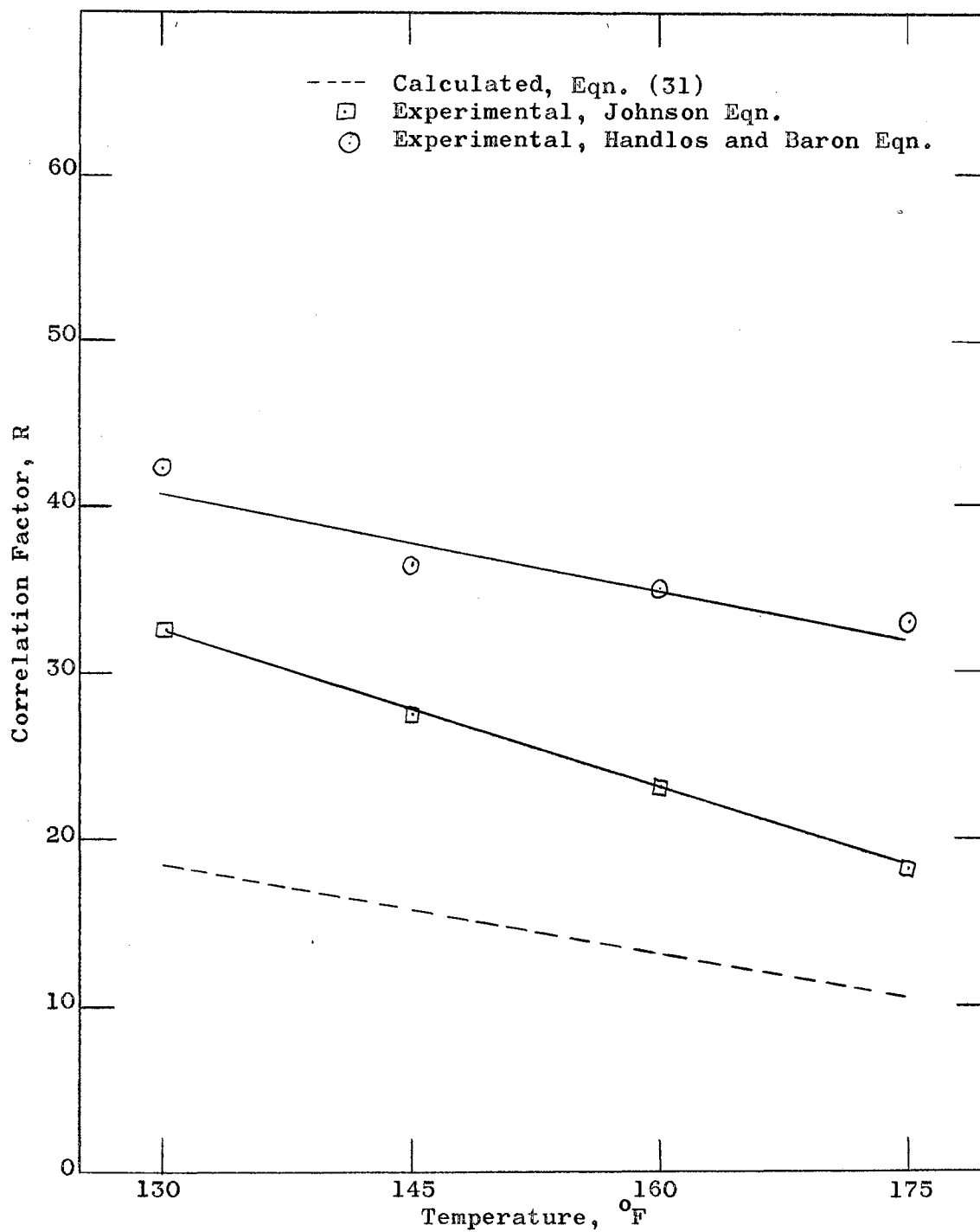


Figure 10, Effect of Temperature on the Correlation Factor, R , for the System Phenol--Cetane + Xylene

Dimensionless Correlation

Many mechanisms have been proposed for mass transfer during free rise or fall. Most investigators agree that the rate of mass transfer is dependent upon the degree of internal circulation within the drop. Therefore, the mechanisms proposed by the various investigators are usually good only in the circulation regime in which their data were taken.

Since there is no quantitative method of measuring the internal circulation of a drop, many investigators have tried to correlate mass transfer rates against various physical and chemical properties. The dimensionless correlation seems to be the most promising method for predicting mass transfer rates.

Garner (7) found that the exponent of the Schmidt number was a function of the degree of circulation within a drop. The Schmidt number has an exponent of 1/2 for complete mixing and an exponent of 1/3 for stagnant drops. The correlation of Garner was

$$Sh = - 126 + 1.8 Re^{0.5} Sc^{0.42} \quad (28)$$

Hurst (15) found that the inclusion of the Weber number helped his correlation. The correlation of Hurst was

$$Sh = - 610 + 0.46 Re^{0.5} Sc^{0.47} We^{0.9} \quad (29)$$

In this work the assumption was made that all the resistance to mass transfer was in the drop. This was a reasonable assumption, since the phases were mutually saturated. This reduces the resistance of the continuous phase to transfer.

In this work two correlations of the type proposed by Garner

were required, one for the systems of pure cetane--phenol and phenol + xylene--cetane, and the other for the system cetane + xylene--phenol. These two correlations had different exponents on the Schmidt number. The Schmidt number is a ratio of the momentum diffusivity to molecular diffusivity. A change in the exponent of the Schmidt number should, therefore, indicate different degrees of circulation within the drop. It was also found that in this work the correlation was not helped by the inclusion of the Weber number.

The correlation obtained for the cetane--phenol and the phenol + xylene--cetane system was

$$Sh = - 75 + 1.19 Re^{0.5} Sc^{0.4} \quad (34)$$

The largest deviation from this was 5.25%, and the average deviation was 2.23%.

The correlation obtained for the cetane + xylene--phenol system was

$$Sh = - 35 + 0.833 Re^{0.5} Sc^{0.43} \quad (35)$$

The largest deviation from this was 5.82% and the average deviation was 2.9%. Kim's (19) data for pure cetane was found to fit this correlation within 6%. His data for 1-methylnapthalene seemed to follow a third correlation.

$$Sh = -92 + 1.1 Re^{0.5} Sc^{0.4} \quad (36)$$

Figures 11 and 12 show the correlations found in this study. Thorsen and Terjesen (34) felt that boundary layer separation,

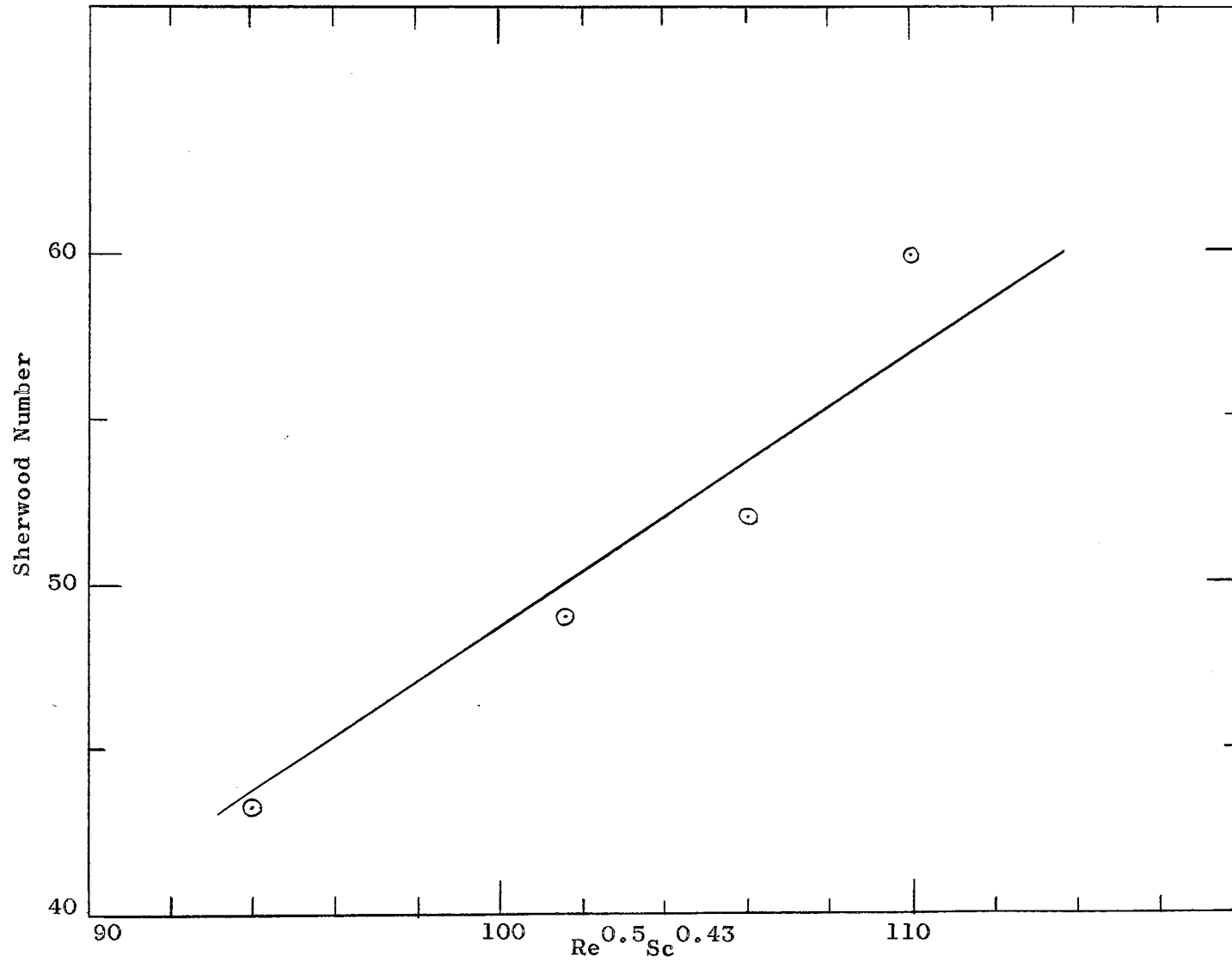


Figure 11, Dimensionless Correlation for the System Phenol--Cetane + Xylene

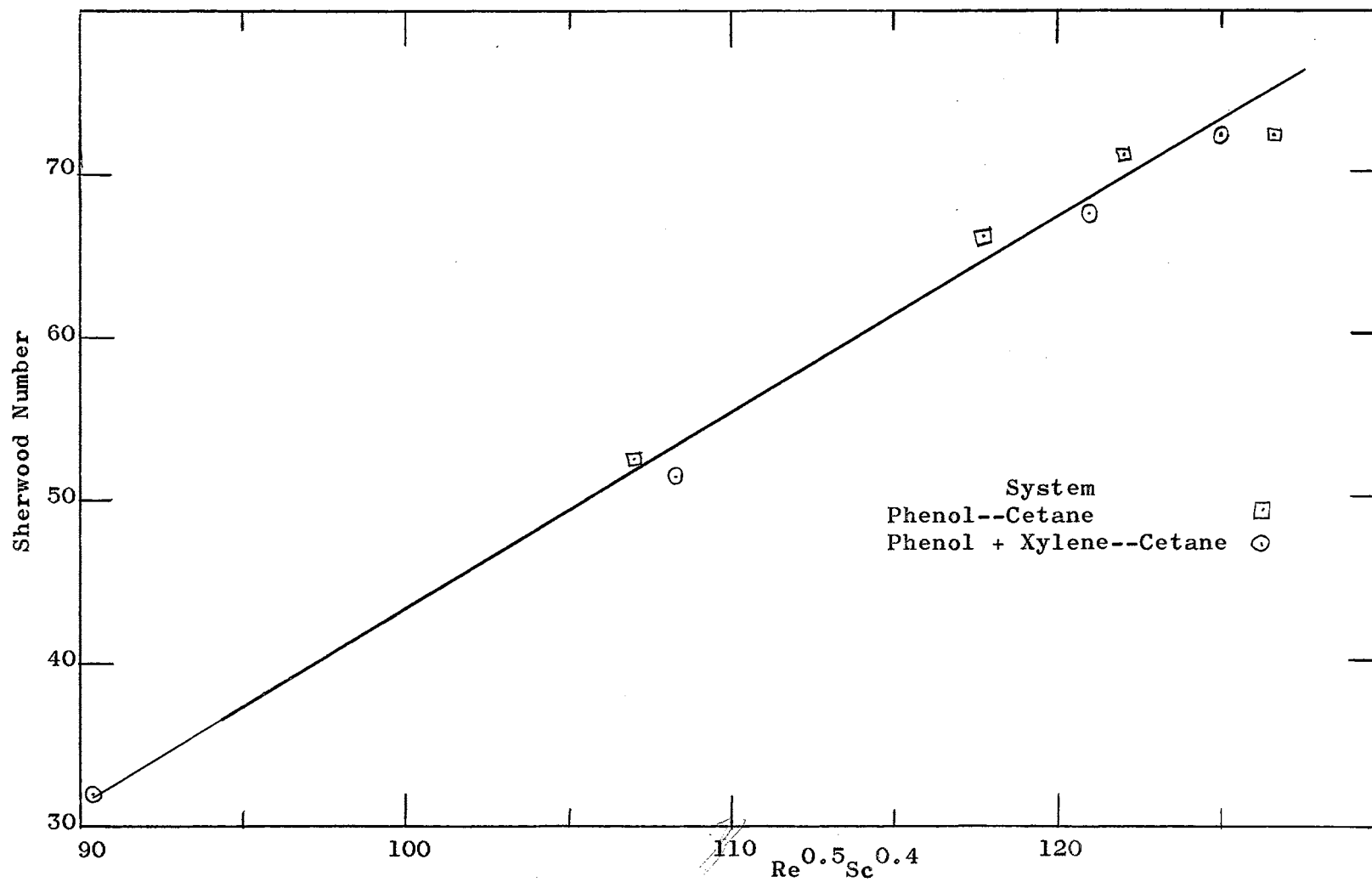


Figure 12, Dimensionless Correlation for the Systems Phenol--Cetane and Phenol + Xylene--Cetane

not internal circulation, was responsible for the large mass transfer rates in liquid drops. They found that this separation occurred at Re of 17, and for all drops with a Reynolds number greater than 17 the Schmidt number should have an exponent of $1/3$. The data from this work was found to be at the lower limit of Sherwood numbers, where Thorsen and Terjesen had very little data. The data from this work seems to fit their line, but was still in three separate groups. This would indicate that, at least for low Sherwood numbers, the direction of solute transfer is important. Thorsen and Terjesen's correlation was

$$Sh = -178 + 3.62 Re^{0.5} Sc^{0.33} \quad (30)$$

Most of their work was with Sherwood numbers between 500 and 800. The Sherwood numbers for this work were below 100. Figure 13 shows the data from this work on their line.

Lileeva and Smirnov (27) analyzed the equations of motion, continuity, and diffusion with the proper initial and boundary conditions to find the important variables in mass transfer from liquid spheres. They found that their data fitted the equation

$$Ki = 3.79 \times 10^{-9} Re^{.5} Ar^2 Fo^{.42} \phi^{-.7} Pr_d^{.5} Pr_c^{.5} m^{-.5} \Gamma^{-1.5} \quad (23)$$

The data from this work was correlated against their work by plotting Ki against $Re^{.5} Ar^2 Fo^{.42} \phi^{-.7} Pr_d^{.5} Pr_c^{.5} m^{-.5} \Gamma^{-1.5}$. The data for the transfer of xylene in both directions fell along the line

$$Ki = 120 - 1.67 \times 10^{-6} Re^{.5} Ar^2 Fo^{.42} \phi^{-.7} Pr_d^{.5} Pr_c^{.5} m^{-.5} \Gamma^{-1.5} \quad (37)$$

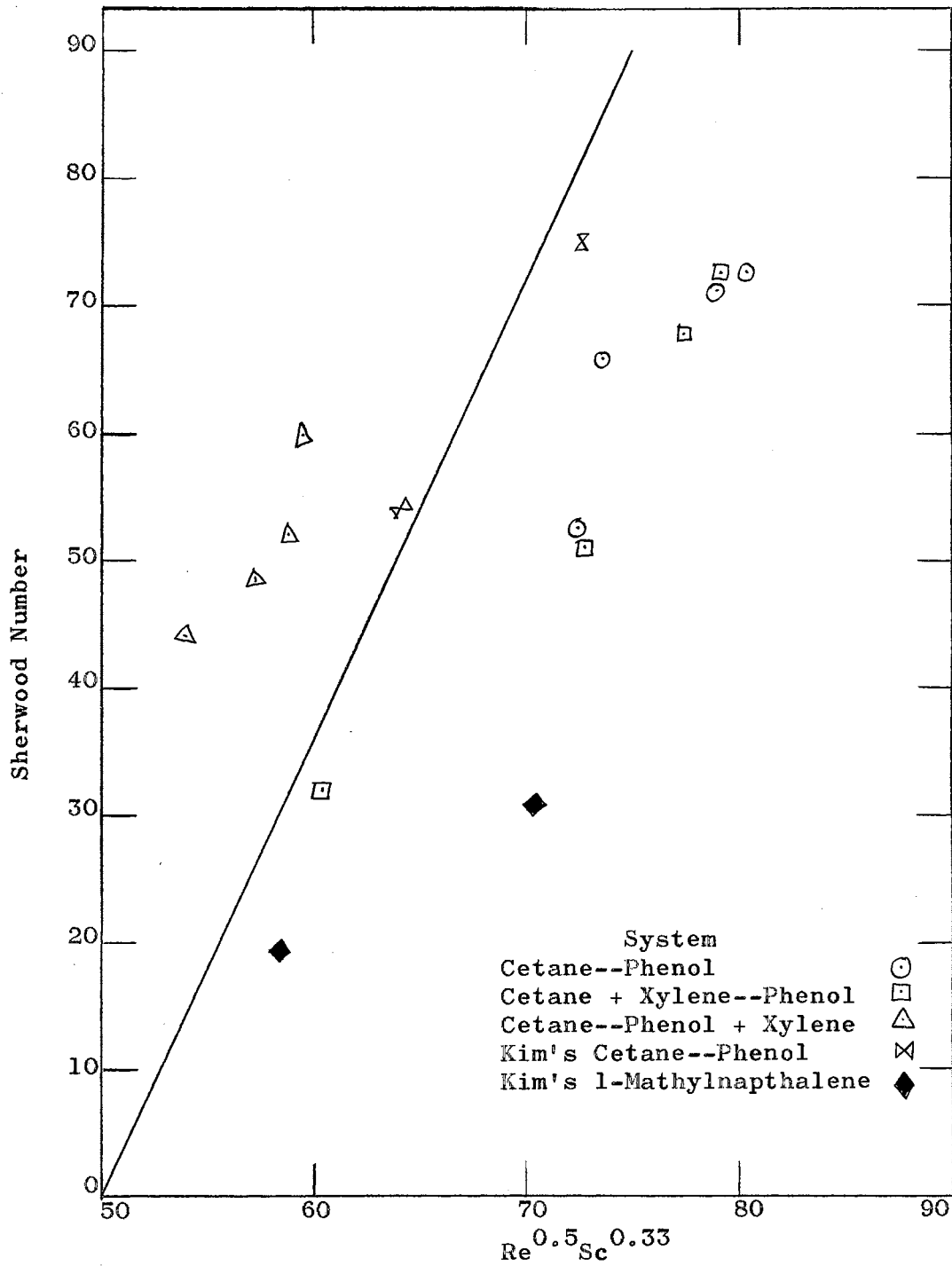


Figure 13, Dimensionless Correlation Proposed by Thorsen and Terjesen

As seen in Figure 14, this line has a negative slope, where Lileeva and Smirnov's line had a positive slope. It is possible that a sign on one of the exponents may have been changed in the translation.

The data for the solubility of phenol in cetane did not follow this line, but was much higher. The diffusivities were calculated by the Wilke equation, which may not be valid for solute molecules as large as cetane.

The extraction data at high temperature were correlated with the same equations used for low temperature data. This would indicate that temperature affects extraction only by its effect on the physical and chemical properties of the system.

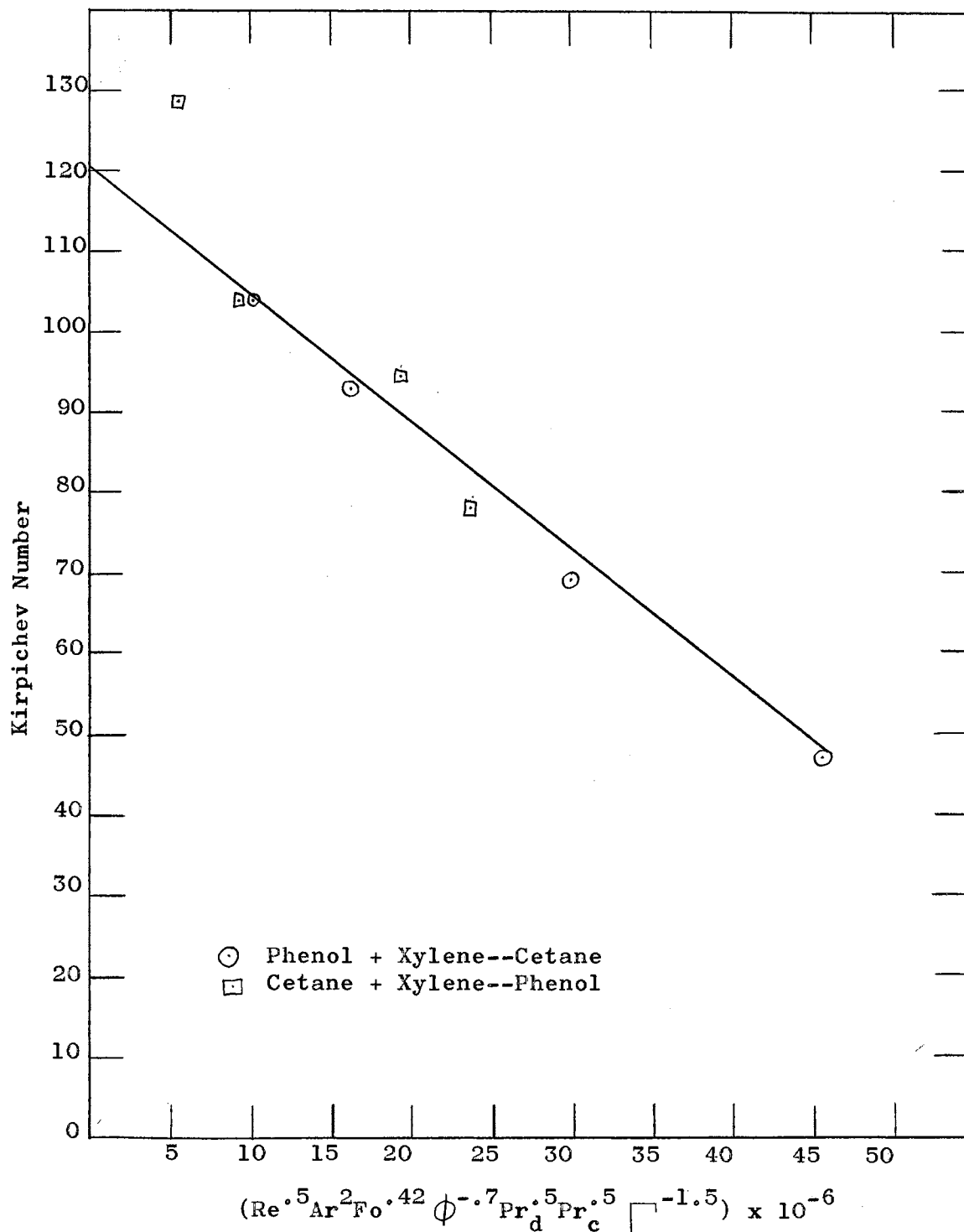


Figure 14, Dimensionless Correlation Using Exponents Suggested by Lileeva and Smirnov

CHAPTER V

CONCLUSIONS AND RECOMMENDATIONS

Restatement of the Problem

A study of mass transfer from single drops was conducted at several temperatures in order to determine the effect of temperature on mass transfer rates. The mass transfer rates were to be correlated in terms of physical and chemical properties.

Conclusions

Oscillations of the rise path were observed visually in the drops used in this study. The Reynolds numbers found in this study were lower than those of other investigators reporting droplet oscillation. This would suggest that at high temperatures, oscillations may be affected by more than the Reynolds numbers.

End Effects

The total end effects observed in this study were compared with the total end effects predicted by Johnson's (17) equation. Johnson's equation predicted end effects which were always higher than the experimental and sometimes went over 100%. In this connection, more high temperature work should be done on end effects. The end effect transfer efficiencies increased with increasing temperature.

Free Rise

The mass transfer efficiencies for free rise did not fit any of the proposed mechanisms. The Handlos and Baron (5) model predicted transfer efficiencies which were up to 50% too high, and the Kronig and Brink model predicted transfer efficiencies which were from 13.5 to 35% too low. This was not too surprising, since each of these models represents a particular regime of internal drop circulation. The free rise transfer efficiencies increased with increasing temperature over the temperature range studied.

Dimensionless Correlation

Of all the proposed dimensionless correlations, the data from this work seemed to fit the correlation of Thorsen and Terjesen (34) the best. The data still fell into groups, depending upon the solute and the direction of the solute transfer. This would indicate that, at least for low Sherwood numbers, the direction of transfer and the type of solute are important.

Recommendations

Future Studies

A complete end effects study should be done at higher temperatures, in order to establish or reject the proposed mechanisms for end effect transfer. If possible, a dimensionless correlation for end effect transfer should be proposed.

Free rise studies should be continued at higher temperatures, especially at high Sherwood numbers. Also, many types of solute should be used. This would test Thorsen and Terjesen's (34)

correlation. A much greater temperature range should be studied to determine the effect of temperature on transfer efficiencies.

Equipment Alteration

The present equipment should be redesigned, extending the jacket to completely enclose the sampling tube. This would eliminate temperature gradients in the sample.

Another high-temperature column should be designed with two coalescence areas. This would allow the end effects to be broken up into formation and coalescence effects.

A SELECTED BIBLIOGRAPHY

1. Baird, M.H.I., and Hamielec, A.E., "Forced Convection Transfer Around Spheres at Intermediate Reynolds Numbers," Can. J. Chem. Engr., 40, 119 (1962).
2. Calderbank, P.H., and Korchinski, J.O., "Circulation in Liquid Drops," Chem. Eng. Sci., 6, 68 (1956).
3. Constan, G.L., and Calvert, S., "Mass Transfer in Drops Under Conditions That Promote Oscillation and Internal Circulation," Preprint 35, A.I.Ch.E., Dec. 2-7, 1961
4. Elgin, J.C., and Browning, F.M., "Extraction of Acetic Acid With Isopropyl Ether In a Spray Column," Transactions of A.I.Ch.E., 31, 639 (1935).
5. Elzinga, E.R., and Banchemo, J.I., "Some Observations on the Mechanics of Drops in Liquid-Liquid Systems," A.I.Ch.E. Journal, 7, 395 (1961).
6. Friedlander, S.K., "A Note on Transport to Spheres in Stokes Flow," A.I.Ch.E. Journal, 7, 347 (1961).
7. Garner, F.H., Foord, A., and Tayeban, M., "Mass Transfer From Circulating Liquid Drops," Journal of Applied Chemistry, 9, 315 (1959).
8. Garner, F.H., and Hale, A.R., "Solute Transfer To and From Liquid Drops," Journal of Applied Chemistry, 5, 653 (1955).
9. Garner, F.H., and Skelland, A.H.P., "Mechanism of Solute Transfer From Droplets," Ind. Eng. Chem., 46, 1255 (1954).
10. Handlos, A.E., and Baron, T., "Mass and Heat Transfer From Drops in Liquid-Liquid Extraction," A.I.Ch.E. Journal, 3, 127 (1957).
11. Haydon, D.A., "An Investigation of Droplet Oscillation During Mass Transfer," Royal Society of London Proceedings, A-243, 483 (1958).
12. Heertjes, P.M., Holve, W.A., and Talsma, H., "Mass Transfer Between Iso-BuOH and Water in a Spray Column," Chem. Eng. Sci., 3, 122 (1954).

13. Higbie, Ralph, "The Rate of Absorption of a Pure Gas Into a Still Liquid During Short Periods of Exposure," Trans. A.I.Ch.E., 31, 365 (1935).
14. Hu, Shengen, and Kintner, R.C., "The Fall of Single Liquid Drops Through Water," A.I.Ch.E. Journal, 1, 42 (1955).
15. Hurst, O.V., Jr., "Solute Transfer From Single Droplets In Liquid-Liquid Extraction," Master's Thesis, Oklahoma State University.
16. Johnson, H.F., and Bliss, H., "Liquid-Liquid Extraction In Spray Towers," Trans. A.I.Ch.E., 42, 331 (1946).
17. Johnson, A.I., and Hamielec, A.E., "Mass Transfer Inside Drops," A.I.Ch.E. Journal, 6, 145 (1960).
18. Johnson, A.I., Hamielec, A., Ward, D., and Golding, A., "End Effect Corrections In Heat and Mass Transfer Studies," Can. J. Chem. Engr., 36, 221 (1958).
19. Kim, W.J., "Phase Equilibrium Data and Extraction Kinetics In the 95 Per Cent Aqueous Phenol--Cetane--1-Methylnapthalene System," Master's Thesis, Oklahoma State University.
20. Klee, A.J., and Treybal, R.E., "Rate of Rise or Fall of Liquid Drops," A.I.Ch.E. Journal, 2, 444 (1956).
21. Kronig, R., and Brink, J., "Theory of Extraction From Falling Drops," App. Sci. Res., A-2, 142 (1950).
22. Lewis, J.B., and Pratt, H.R.C., "Oscillating Droplets," Nature(London), 171, 1155 (1953).
23. Licht, W., and Conway, J.B., "Mechanism of Solute Transfer In Spray Towers," Ind. Eng. Chem., 42, 1151 (1950).
24. Licht, W., and Narasimhamurty, G.S.R., "Rate of Fall of Single Drops," A.I.Ch.E. Journal, 1, 366 (1955).
25. Licht, W., and Pansing, W.F., "Solute Transfer From Single Drops In Liquid-Liquid Extraction," Ind. Eng. Chem., 45, 1885 (1953).
26. Lileeva, A.K., and Smirnov, N.I., "Critical Equations For the Extraction Process," J.App. Chem. of U.S.S.R., 34, 1103 (1961).
27. Lileeva, A.K., and Smirnov, N.I., "Extraction From Single Drops," J. App. Chem. of U.S.S.R., 34, 1295 (1961).
28. McDowell, R.V., and Myers, J.E., "Mechanism of Heat Transfer to Liquid Drops," A.I.Ch.E. Journal, 2, 384 (1956).

29. Newman, A.B., "The Drying of Porous Solids: Diffusion and Surface Emission Equations," Trans. A.I.Ch.E., 27, 203 (1931).
30. Null, H.R., and Johnson, H.F., "Drop Formation in Liquid-Liquid Systems From Single Nozzles," A.I.Ch.E. Journal, 4, 273 (1958).
31. Reid, R.C., and Sherwood, T.K., The Properties of Gases and Liquids, McGraw-Hill Book Co., New York (1958).
32. Sherwood, T.K., Evans, J.E., and Longcor, J.V.A., "Extraction In Spray and Packed Column," Ind. Eng. Chem., 31, 1144 (1939).
33. Strom, J.R., and Kintner, R.C., "Wall Effects For the Fall of Single Drops," A.I.Ch.E. Journal, 4, 153 (1958).
34. Thorsen, G., and Terjesen, S.G., "On the Mechanism of Mass Transfer In Liquid-Liquid Extraction," Chem. Eng. Sci., 17, 137 (1962).
35. Vermeulen, T., "Theory for Irreversible and Constant-Pattern Solid Diffusion," Ind. Eng. Chem., 45, 1664 (1953).
36. West, Frank B., Robinson, P.A., Morgenthaler, A.C., Beck, T.R., and McGregor, D.K., "Liquid-Liquid Extraction From Single Drops," Ind. Eng. Chem., 43, 234 (1951).

APPENDIX A

DEFINITION OF TERMS

- A_i - Interfacial area at coalescence, cm^2
 Ar - Archimedes number, $\frac{d^3 \rho_c g (\rho_c - \rho_d)}{u^2}$
 B - Coefficient
 C - Concentration of the dispersed phase
 d - Drop diameter, cm .
 D - Molecular diffusivity, cm^2/sec .
 E - Transfer efficiency
 Fo' - Fourier diffusion number, $\frac{\Theta D_c}{d^2}$
 g - Gravitational constant
 K - Overall mass transfer coefficient, cm/sec .
 Ki - Kirpichev diffusion number $\frac{Kd}{D_c}$
 Pe' - Modified Peclet number, $Pe / (1 - \frac{u_d}{u_c})$
 Pr' - Prandtl diffusion number, $\frac{u}{De}$
 R - Dimensionless correlation factor
 r - Drop radius
 Re - Reynolds number, dVe/u
 Sc - Schmidt number, u/De
 Sh - Sherwood number, Kd/D
 t - Time

- V - Velocity, cm./sec.
 v - Drop volume, cm³
 We - Weber number, $d v^2/\sigma$

Greek Letters

- \square - Criterion of geometrical similarity
 Θ - Time
 λ - Eigenvalue
 μ - Viscosity, centipoise
 ρ - Density, gm/cm³
 σ - Interfacial tension, dynes/cm.
 ϕ - Phase volume ratio, v_c/v_d

Subscripts

- 1 - In the nozzle
 2 - Beginning of transfer mechanism during free-rise
 3 - Point at which drop strikes coalesced dispersed phase
 4 - At column outlet
 c - Continuous phase
 c - Coalescence
 d - Dispersed
 E - Combined end effects
 f - Formation
 i - Interfacial
 m - Free-rise

APPENDIX B

PHASE EQUILIBRIUM DATA

This appendix is a description of the experimental apparatus, the procedure used, and the results obtained in the determination of the phase equilibrium data needed for the extraction calculations.

Experimental Apparatus

The apparatus used to obtain the phase equilibrium data was very simple. It consisted of a 125 cc Erlenmeyer flask, a 250 cc beaker, two magnetic stirring bars, and a combination hot plate and magnetic stirrer. The hot plate was covered with a 2 inch thick piece of cork board, which had a hole in the center where the beaker was placed. The beaker was filled with heating oil, and one of the stirring bars was placed in the beaker. The other stirring bar was placed in the flask along with the sample. The flask was then positioned into the beaker in such a manner that both of the bars stirred their respective solutions when the magnetic stirrer was on. In this manner the phases were intimately mixed while kept at a constant temperature.

Experimental Procedure

A clean, dry, 125 cc Erlenmeyer flask was tared on the Mettler

balance. Twenty milliliters of phenol were added, and the flask was weighed. Twenty milliliters of cetane were added, and the flask was weighed again. Varying amounts of o-xylene were added for each run, and the flask was again weighed. The weight per cent of each component in the charge was then calculated.

The stirring bar was then added, and the flask was tightly sealed with a rubber stopper. The flask was positioned in the beaker as described above, and both the stirrer and the heater were started. The solution was brought to the desired temperature and held to within 1°F for two hours. Manual control of the heater was necessary to maintain the temperature within these limits.

After two hours the stirrer was stopped and the two phases were allowed to separate. Ten milliliters of each phase was then transferred to tared weighing bottles by the use of heated pipets.

The samples were weighed on the Mettler balance, and then poured into separatory funnels. Ten milliliters of 20% NaOH solution was added, and the solutions were shaken for ten minutes. The weighing bottles were washed with another ten milliliters of the NaOH solution, which was added to the separatory funnel.

The oil in the sample was then transferred to other weighing bottles and weighed. The differences in weight were the weights of the phenol in the two samples. The oil from each phase was analyzed by refractive index, giving the composition of each phase. The weight per cents were plotted on triangular graph paper. The analysis could then be checked by just looking at

the graph, since the charge and the two end points must all lie on the same tie line.

The Plait point was estimated by making conjugate lines, and drawing the conjugate curve through the phase boundary curve.

TABLE III

EQUILIBRIUM AND PHASE BOUNDARY DATA FOR THE 95% AQ.

PHENOL-CETANE-O-XYLENE SYSTEM AT 130°F.

Charge			Upper Phase Composition			Lower Phase Composition		
A	B	C	A	B	C	A	B	C
0.578	0.422	0.00	0.0566	0.9434	0.00	0.953	0.047	0.00
0.544	0.393	0.063	0.0665	0.838	0.0755	0.9107	0.0509	0.0384
0.5338	0.3804	0.0858	0.112	0.795	0.093	0.890	0.055	0.055
0.512	0.371	0.117	0.0993	0.7665	0.1342	0.845	0.0662	0.0888
0.478	0.346	0.176	0.137	0.667	0.196	0.774	0.137	0.189

Component A, 95% aq. phenol

Component B, Cetane

Component C, O-Xylene

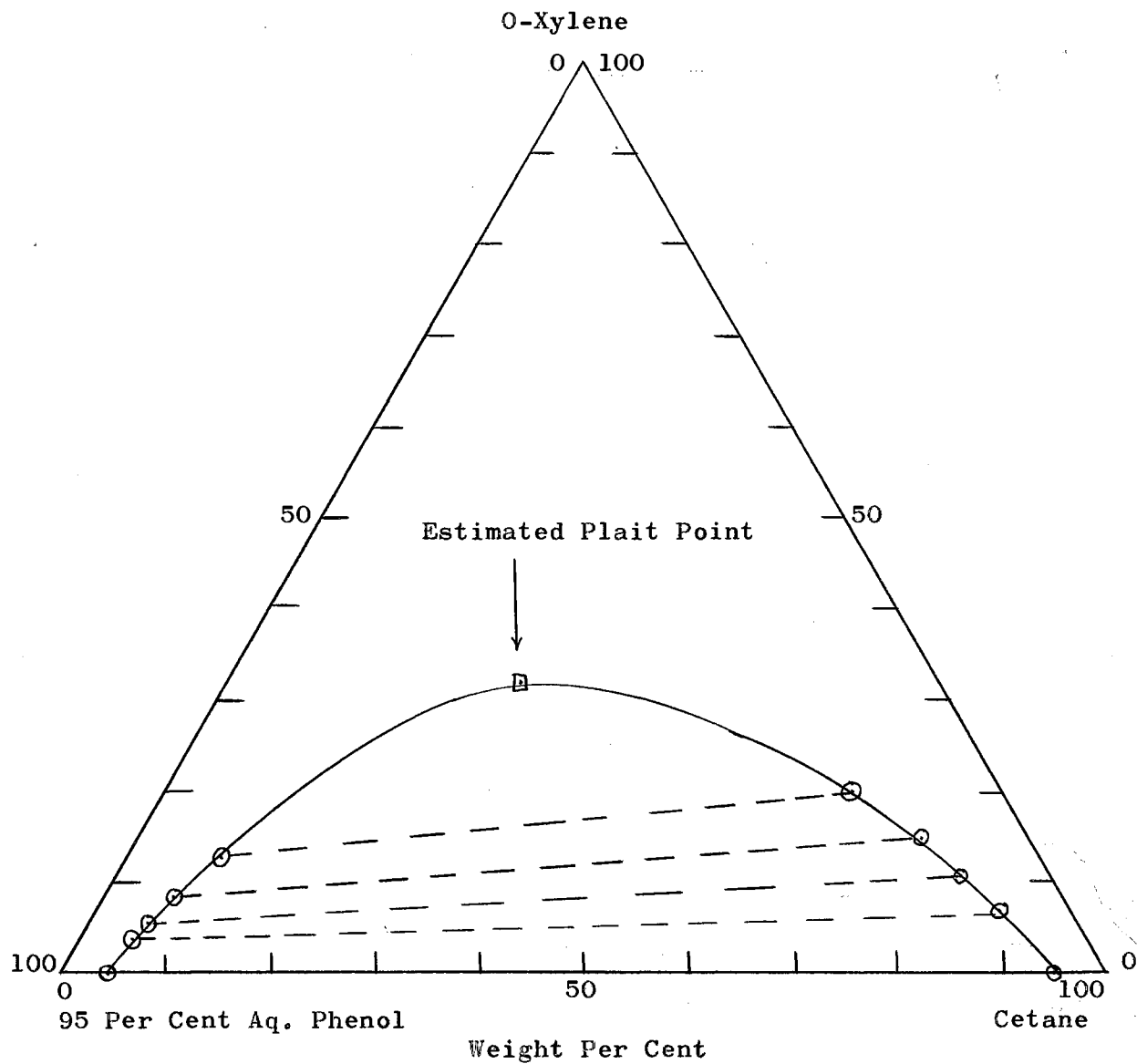


Figure 15, Ternary Diagram for the 95 Per Cent Aq. Phenol--Cetane--
O-Xylene System at 130°F

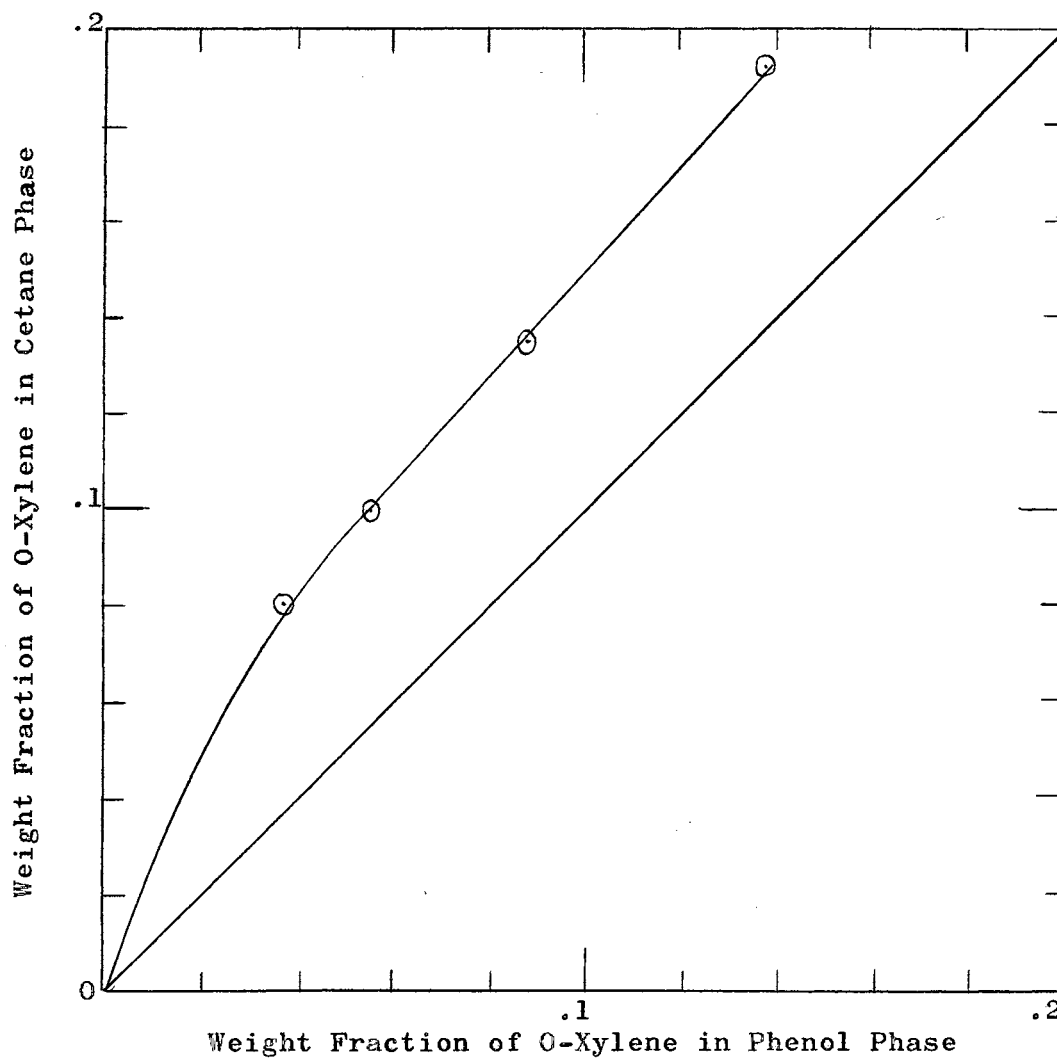


Figure 16, Distribution Data of O-Xylene Between Cetane and 95% Aq. Phenol at 130°F

TABLE IV

EQUILIBRIUM AND PHASE BOUNDARY DATA FOR THE 95% AQ.

PHENOL-CETANE-O-XYLENE SYSTEM AT 145°F.

Charge			Upper Phase Composition			Lower Phase Composition		
A	B	C	A	B	C	A	B	C
0.577	0.423	0.00	0.0791	0.9209	0.00	0.95	0.05	0.00
0.5564	0.404	0.0396	0.103	0.8464	0.0506	0.9326	0.0476	0.0198
0.530	0.381	0.0887	0.1305	0.7912	0.0783	0.881	0.0613	0.0577
0.5017	0.3633	0.135	0.155	0.701	0.144	0.806	0.087	0.107
0.4890	0.353	0.158	0.201	0.638	0.161	0.784	0.120	0.096

Component A, 95% aq. phenol

Component B, Cetane

Component C, O-Xylene

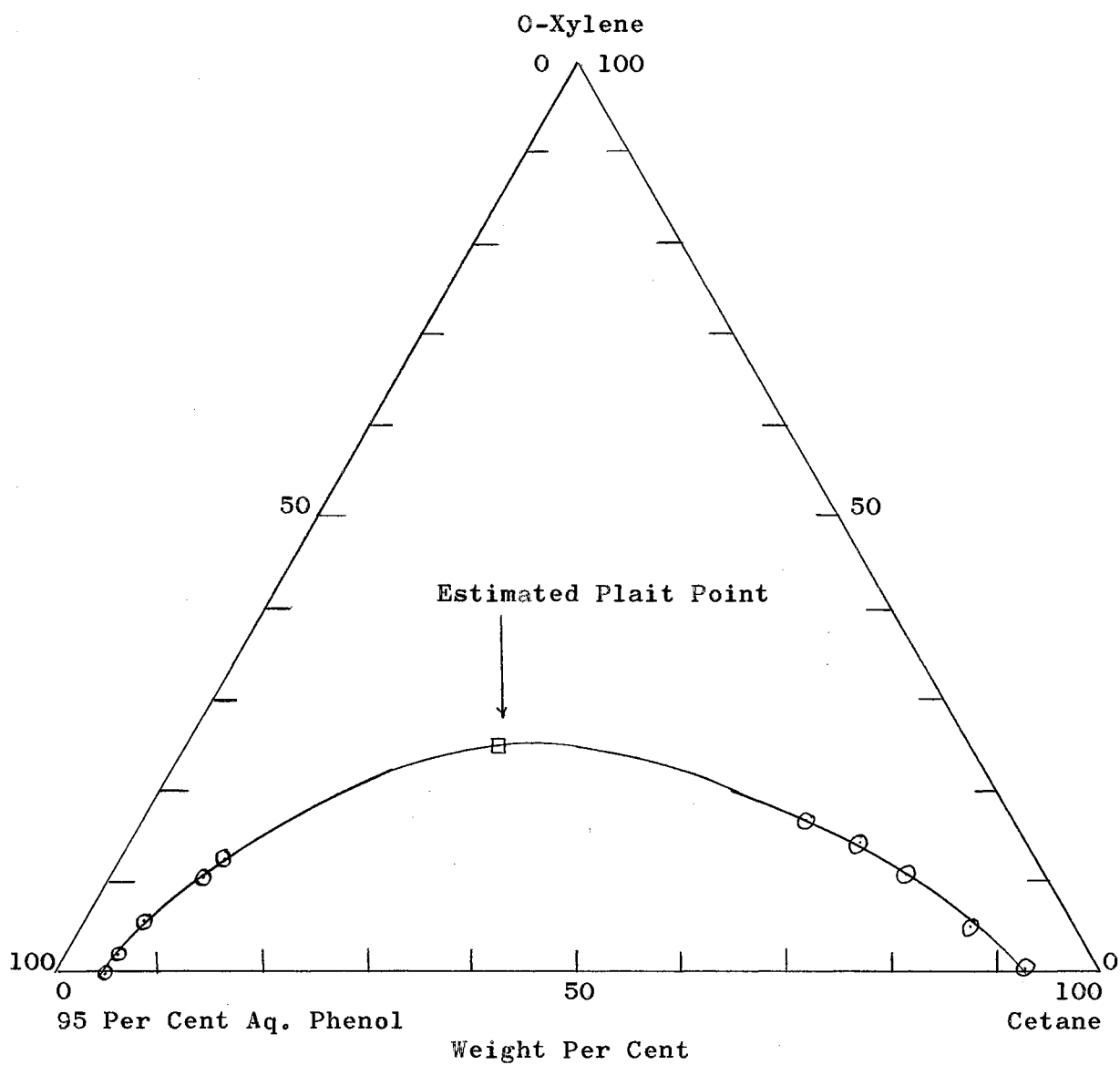


Figure 17, Ternary Diagram for the 95 Per Cent Aq. Phenol--Cetane--O-Xylene System at 145°F

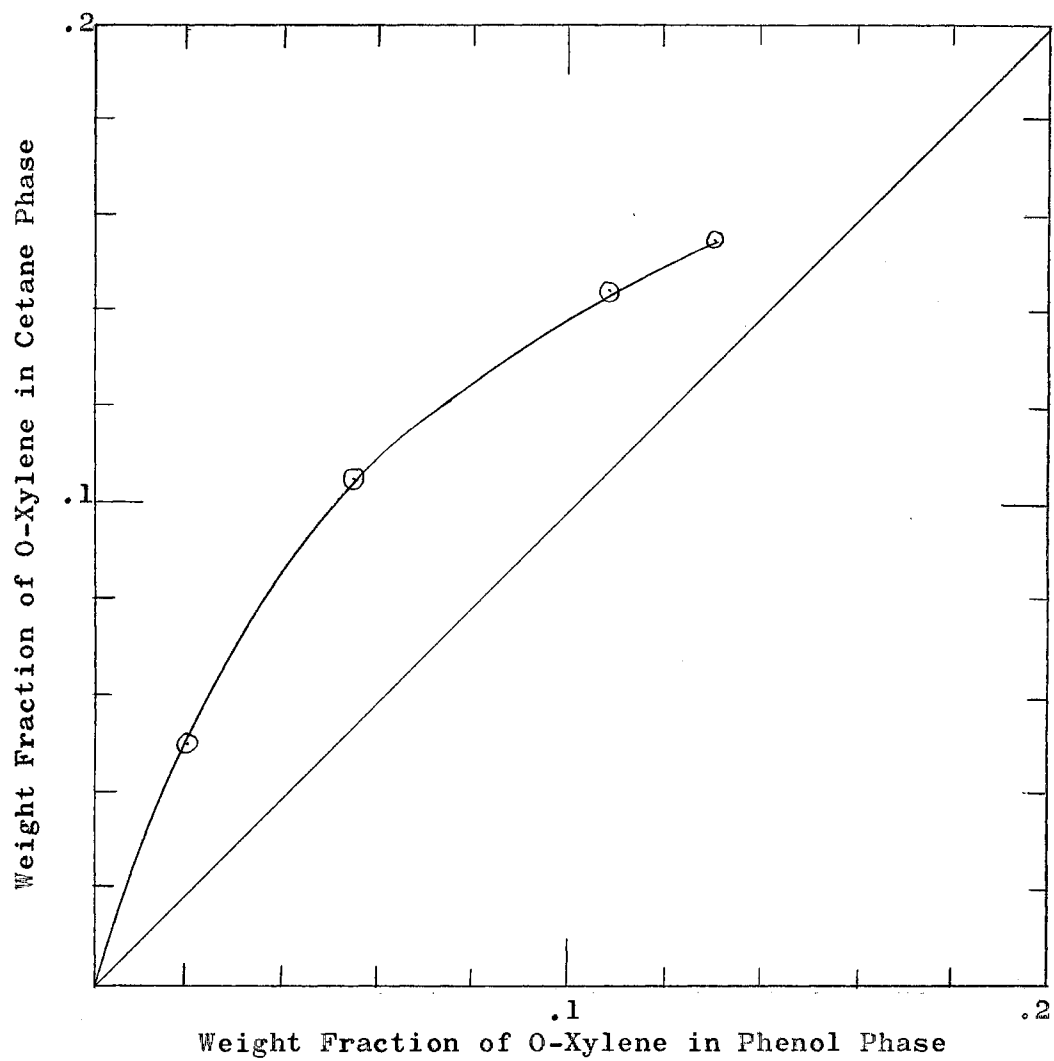


Figure 18, Distribution Data of O-Xylene Between Cetane and 95 Per Cent Aq. Phenol at 145°F

TABLE V

EQUILIBRIUM AND PHASE BOUNDARY DATA FOR THE 95% AQ.

PHENOL-CETANE-O-XYLENE SYSTEM AT 160°F.

Charge			Upper Phase Composition			Lower Phase Composition		
A	B	C	A	B	C	A	B	C
0.580	0.420	0.00	0.087	0.913	0.00	0.936	0.064	0.00
0.483	0.347	0.170	0.267	0.554	0.179	0.698	0.155	0.147
0.468	0.338	0.196	0.336	0.459	0.205	0.613	0.223	0.164
0.515	0.370	0.115	0.155	0.710	0.135	0.795	0.105	0.100
0.525	0.380	0.095	0.147	0.746	0.107	0.832	0.091	0.077
0.470	0.348	0.192	0.290	0.511	0.199	0.649	0.181	0.170
0.465	0.342	0.192	0.257	0.520	0.223	0.627	0.198	0.175
0.528	0.388	0.089	0.0875	0.821	0.0915	0.854	0.0875	0.0585

Component A, 95% aq. phenol

Component B, Cetane

Component C, O-Xylene

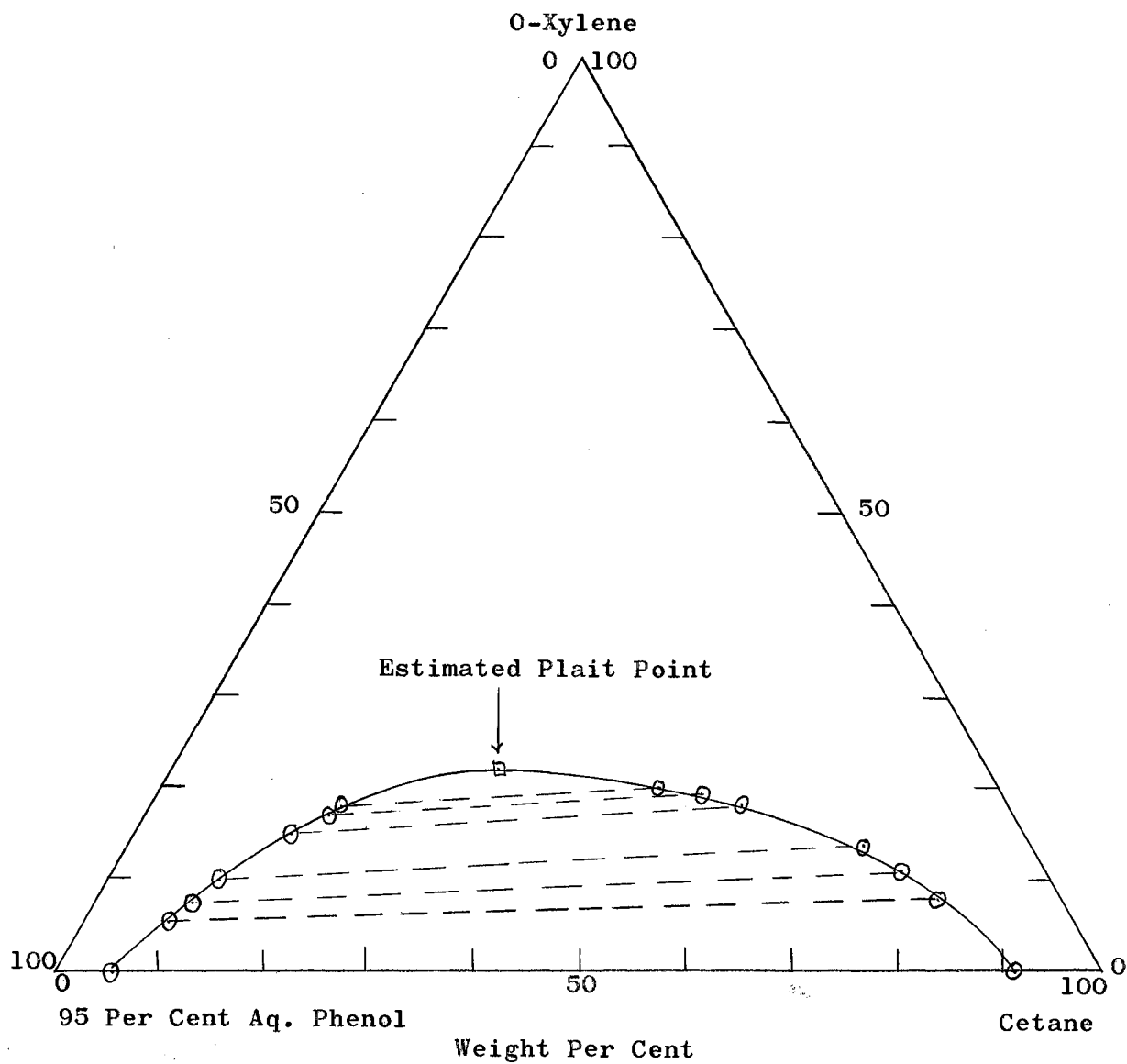


Figure 19, Ternary Diagram for the 95 Per Cent Aq. Phenol--Cetane--O-Xylene System at 160°F.

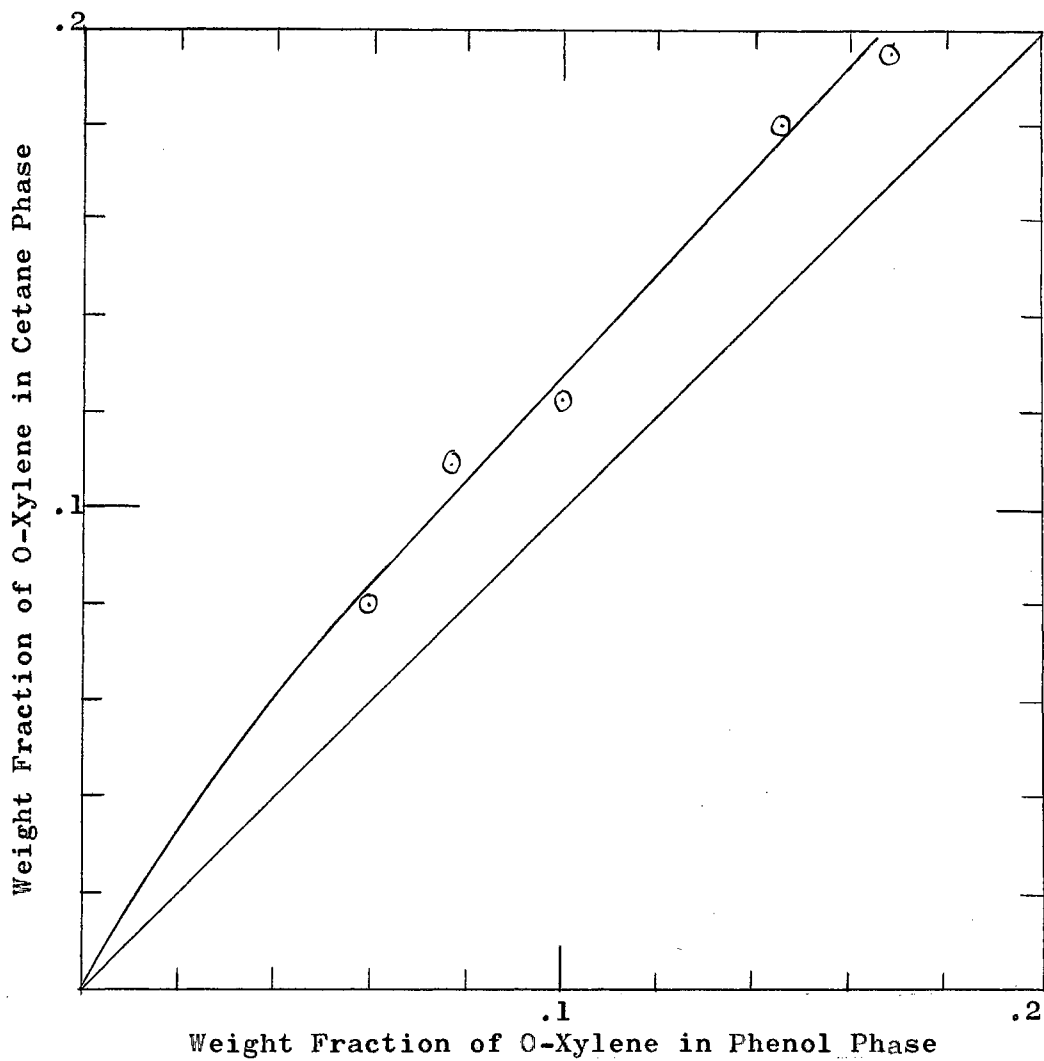


Figure 20, Distribution Data of O-Xylene Between Cetane and 95 Per Cent Aq. Phenol at 160°F

TABLE VI

EQUILIBRIUM AND PHASE BOUNDARY DATA FOR THE 95% AQ.

PHENOL-CETANE-O-XYLENE SYSTEM AT 175°F.

Charge			Upper Phase Composition			Lower Phase Composition		
A	B	C	A	B	C	A	B	C
0.578	0.422	0.00	0.097	0.903	0.00	0.924	0.076	0.00
0.524	0.380	0.096	0.178	0.715	0.107	0.819	0.104	0.077
0.505	0.367	0.128	0.237	0.630	0.133	0.740	0.120	0.140
0.478	0.347	0.175	0.397	0.430	0.173	0.586	0.257	0.157
0.541	0.392	0.067	0.1536	0.771	0.0754	0.853	0.0955	0.0515

Component A, 95% aq. phenol

Component B, Cetane

Component C, O-Xylene

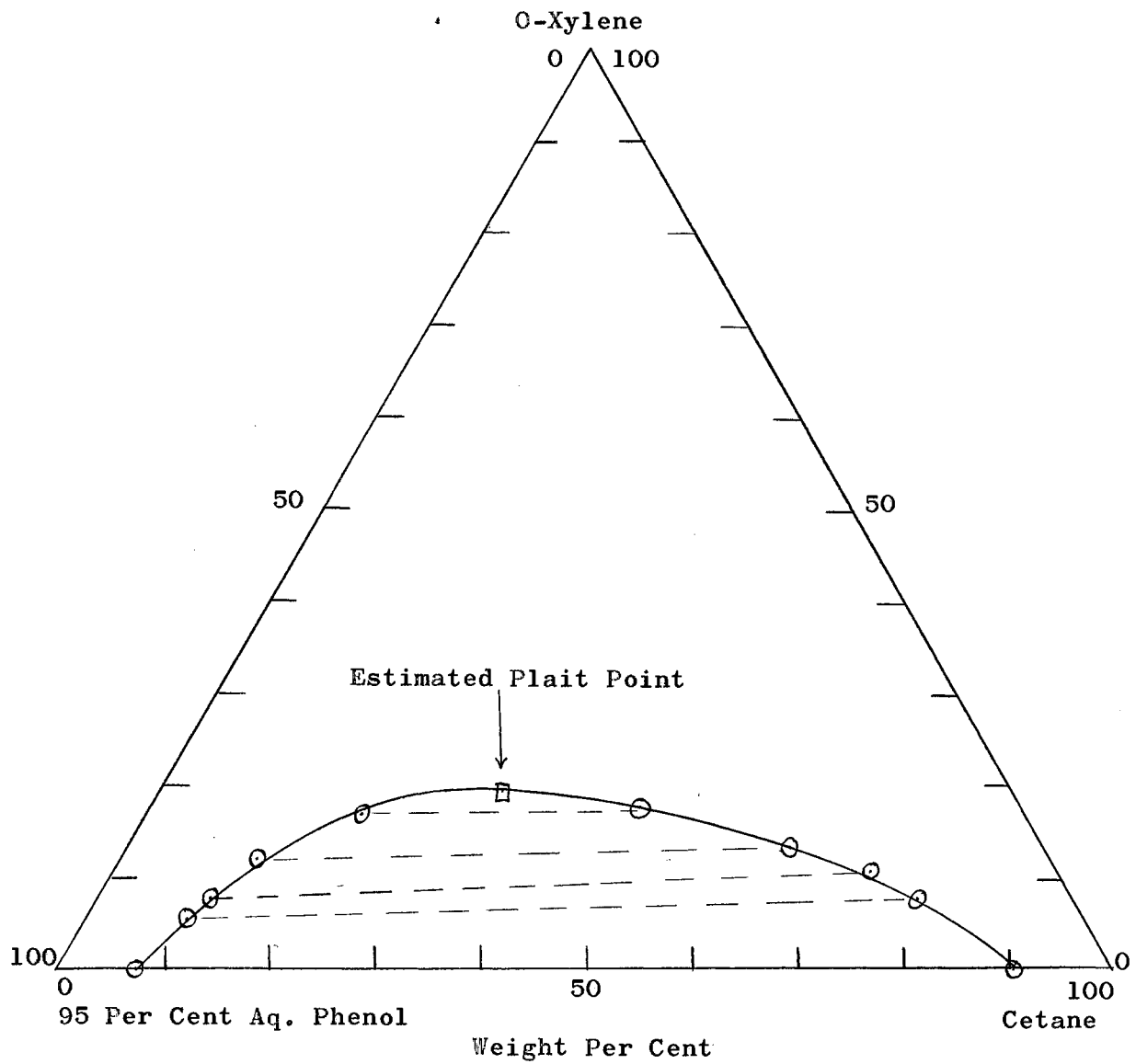


Figure 21, Ternary Diagram for the 95 Per Cent Aq. Phenol--Cetane--
O-Xylene System at 175°F

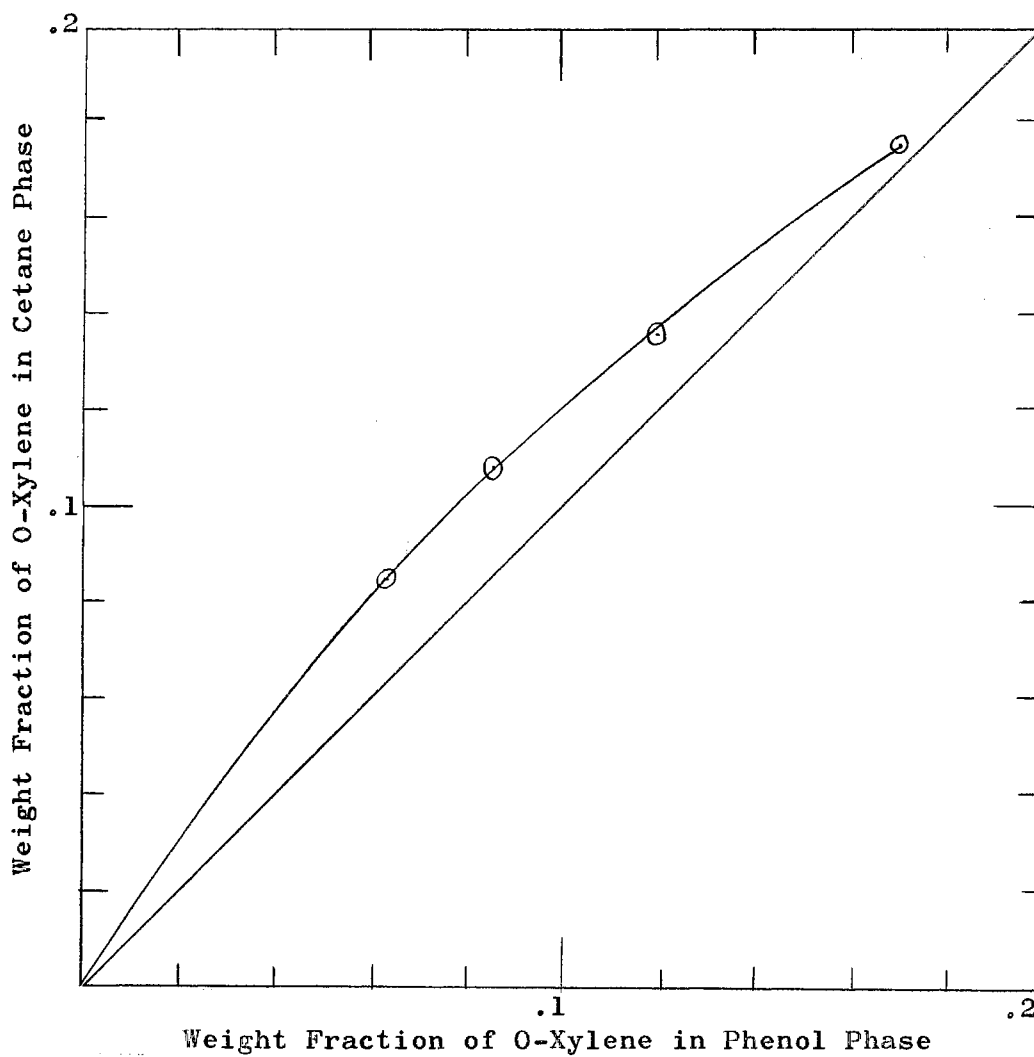


Figure 22, Distribution Data of O-Xylene Between Cetane and 95 Per Cent Aq. Phenol at 175°F

APPENDIX C

PHYSICAL PROPERTIES OF THE EQUILIBRATED PHASES

This appendix is a description of the experimental methods used and the results obtained for the determination of the physical properties of the continuous and dispersed phases. Tables VIII through XII give the experimental results.

Refractive Index-Composition Curve for the

Cetane-O-Xylene System

The points on the refractive index--composition curve were determined by the use of the Spencer 1591 Refractometer. Samples of cetane and xylene were weighed, and the refractive index of the mixture was observed. The weight per cent was calculated for each sample and plotted against the refractive index. Figure 9 shows the refractive index--composition curve used in this work.

Densities of the Equilibrated Phases

Densities of the two phases in each system were determined by the use of two pycnometers. The pycnometers full of solution were placed in a constant temperature bath and allowed to reach equilibrium. The pycnometers were then dried and weighed on the

Mettler balance. Since the volumes of the pycnometers were known, the densities of the solutions could be calculated.

Viscosities of the Equilibrated Phases

The viscosities were measured by the use of Ostwald viscometer. The viscometers were placed in the refractometer bath to hold them at constant temperature. The time of outflow was measured with a stop watch. The viscometers were standardized with water. The viscosities of the phases were calculated by the equation

$$\frac{u_1}{u_2} = \frac{e_1 t_1}{e_2 t_2} \quad (38)$$

where t is the time of outflow.

Interfacial Tension Between the Equilibrated Phases

The interfacial tensions were measured with a Cenco 70535 Ring Tensiometer. The beaker containing the two phases was placed on an insulated hot plate to hold the solution at constant temperature. The ring was pulled from the phenol phase into the cetane phase.

Diffusivities of the Equilibrated Phases

The diffusivities of the two phases were calculated using Wilke's equation as cited by Reid and Sherwood (31).

$$D_{12} = 7.4 \times 10^{-8} \frac{(X M)^{0.5} T}{u V_1^{0.6}} \quad (39)$$

Where:

D_{12} = Diffusion coefficient of solute 1 in dilute solution
solution in solvent 2.

M = Molecular weight of solvent

T = Temperature, $^{\circ}\text{K}$

u = Viscosity of solution, centipoises

V_1 = Molal volume of solute at normal boiling point, cm^3/gm
mole

X = Association parameter of solvent

TABLE VII
REFRACTIVE INDEX--COMPOSITION DATA FOR
THE CETANE--O--XYLENE SYSTEM

<u>Weight Per Cent Cetane</u>	<u>R.I.</u>
62.496	1.4522
39.388	1.4685
72.770	1.4460
53.385	1.4585
45.546	1.4640
18.065	1.4840
84.691	1.4390
23.371	1.4801
13.989	1.4877
100.0	1.4300
0.0	1.5000

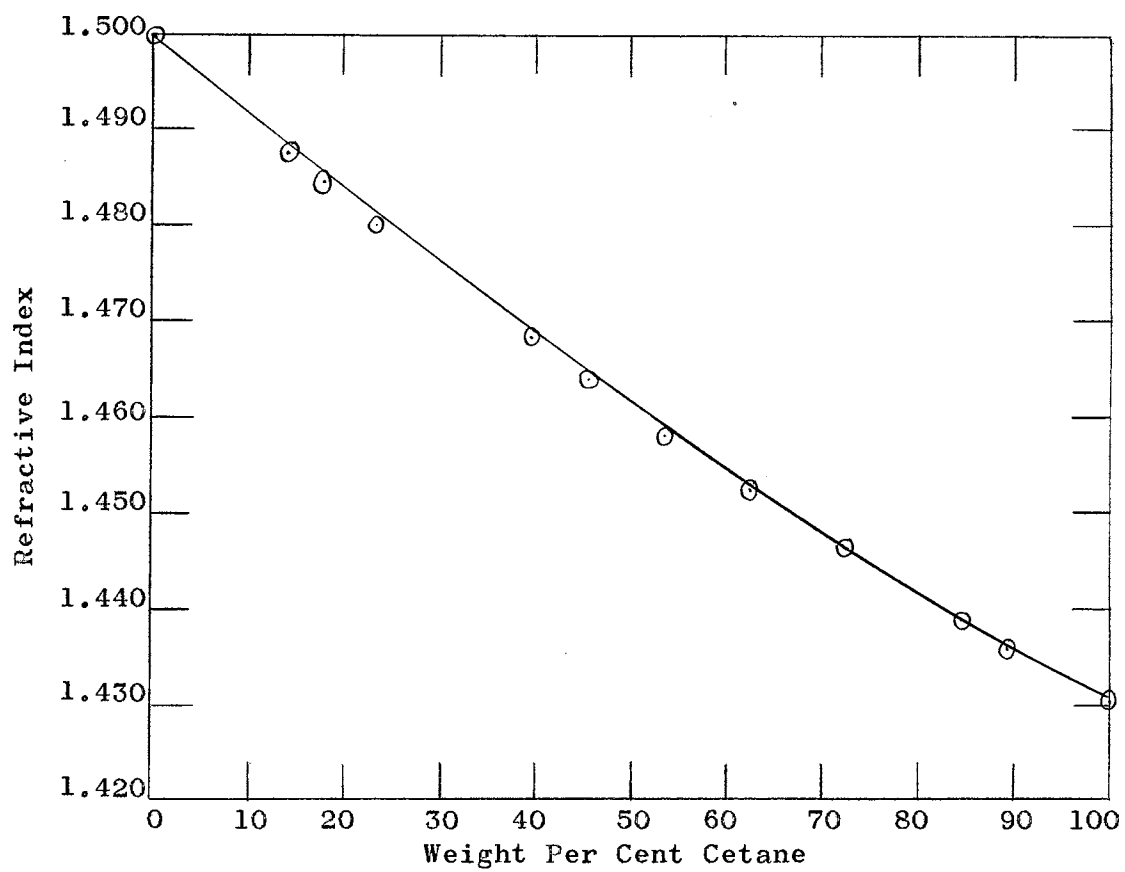


Figure 23, Refractive Index--Composition Curve for the
Cetane--O-Xylene System

TABLE VIII

DENSITIES OF THE EQUILIBRATED PHASES

	<u>Continuous Phase Densities</u>	<u>Dispersed Phase Densities</u>
I. Phenol--Cetane		
130°F	1.0419	0.7493
145°F	1.0351	0.7440
160°F	1.0286	0.7384
175°F	1.0221	0.7332
II. Phenol saturated with cetane with 11.4% xylene--Cetane saturated with phenol		
130°F	1.0086	0.7514
145°F	1.0023	0.7465
160°F	0.9947	0.7407
175°F	0.9871	0.7351
III. Phenol saturated with cetane--80.5% cetane, 19.5% xylene saturated with phenol		
130°F	1.0291	0.7698
145°F	1.0223	0.7640
160°F	1.0147	0.7585
175°F	1.0079	0.7525

TABLE IX

VISCOSITIES OF THE EQUILIBRATED PHASES

<u>Continuous Phase Viscosities,</u> Centipoises		<u>Dispersed Phase Viscosities,</u> Centipoises
I. Phenol--Cetane		
130°F	2.3843	1.617
145°F	1.947	1.439
160°F	1.500	1.239
175°F	1.361	1.114
II. Phenol saturated with cetane with 11.4% xylene--Cetane saturated with phenol		
130°F	1.936	1.595
145°F	1.618	1.397
160°F	1.381	1.213
175°F	1.186	0.9538
III. Phenol saturated with cetane--80.5% cetane, 19.5% xylene saturated with phenol		
130°F	2.196	1.211
145°F	1.821	1.079
160°F	1.537	0.9648
175°F	1.3156	0.8755

TABLE X
INTERFACIAL TENSIONS BETWEEN THE EQUILIBRATED PHASES

<u>System</u>	<u>Interfacial Tensions</u> , Dynes/cm
I. Phenol--Cetane	
130 ^o F	2.8
145 ^o F	2.2
160 ^o F	1.9
175 ^o F	1.5
II. Phenol saturated with cetane with 11.4% xylene--Cetane saturated with phenol	
130 ^o F	1.8
145 ^o F	1.6
160 ^o F	1.35
175 ^o F	0.95
III. Phenol saturated with cetane--80.5% cetane, 19.5% xylene saturated with phenol	
130 ^o F	1.75
145 ^o F	1.50
160 ^o F	.95
175 ^o F	0.55

TABLE XI

DIFFUSIVITIES OF THE EQUILIBRATED PHASES

<u>Continuous Phase Diffusivities,</u>		<u>Dispersed Phase Diffusivities,</u>
cm ² /sec.		cm ² /sec.
I. Phenol--Cetane		
130°F	0.339 x 10 ⁻⁵	1.392 x 10 ⁻⁵
145°F	0.427 x 10 ⁻⁵	1.608 x 10 ⁻⁵
160°F	0.567 x 10 ⁻⁵	1.916 x 10 ⁻⁵
175°F	0.640 x 10 ⁻⁵	2.180 x 10 ⁻⁵
II. Phenol saturated with cetane with 11.4% xylene--Cetane saturated with phenol		
130°F	0.82 x 10 ⁻⁵	1.178 x 10 ⁻⁵
145°F	1.01 x 10 ⁻⁵	1.378 x 10 ⁻⁵
160°F	1.21 x 10 ⁻⁵	1.632 x 10 ⁻⁵
175°F	1.44 x 10 ⁻⁵	2.127 x 10 ⁻⁵
III. Phenol saturated with cetane--80.5% cetane, 19.5% xylene saturated with phenol		
130°F	0.722 x 10 ⁻⁵	1.55 x 10 ⁻⁵
145°F	0.892 x 10 ⁻⁵	1.78 x 10 ⁻⁵
160°F	1.09 x 10 ⁻⁵	2.057 x 10 ⁻⁵
175°F	1.30 x 10 ⁻⁵	2.317 x 10 ⁻⁵

APPENDIX D

EXPERIMENTAL DATA AND CALCULATIONS

This appendix contains the data used and the calculations made in this study. It contains sample calculations of the calculations made.

Sample Calculations

Transfer Efficiencies Calculated by the Kronig and Brink Model

$$E_m = 1 - \frac{3}{8} \sum_{n=1}^{\infty} B_n^2 e^{-\left[\lambda_n \frac{16Dt}{r^2} \right]} \quad (12)$$

$$\lambda_1 = 1.678$$

$$D = 1.39 \times 10^{-5} \text{ cm}^2/\text{sec.}$$

$$\lambda_2 = 9.83$$

$$r = 0.1015 \text{ cm}$$

$$B_1 = 1.32$$

$$t = 3.8 \text{ sec.}$$

$$B_2 = 0.73$$

using the first two terms

$$E_m = 1 - \frac{3}{8}(1.51 + .235)$$

$$E_m = 0.655$$

Calculated Correlation Factor

The correlation factor can be calculated from an equation proposed by Handlos and Baron.

$$R = dV/D (1 + u_d/u_c) 2048 \quad (31)$$

$$R = .203(8.03)/1.39 \times 10^{-5} (1 - 1.617/2.384) 2048$$

$$R = 34.0$$

Experimental Correlation Factor

Using the Handlos and Baron model:

$$R = \frac{d^2}{16 D \Theta} \ln 2 - \ln(1 - E_m) \quad (40)$$

$$d = .203 \text{ cm}$$

$$D = 1.39 \times 10^{-5}$$

$$\Theta = 3.8 \text{ sec}$$

$$1 - E_m = 0.605$$

$$R = \frac{(.203)^2 (.693 + .502)}{16(1.39 \times 10^{-5}) 3.8}$$

$$R = 58$$

Using Johnson's equation:

$$R = \frac{\text{slope}(d^2)}{\lambda^2 D} \quad (41)$$

$$\lambda = 1.678$$

$$\text{slope} = .175$$

$$d = .203 \text{ cm}$$

$$D = 1.39 \times 10^{-5} \text{ cm}^2/\text{sec.}$$

$$\Theta = 3.8 \text{ sec.}$$

$$R = \frac{.175(.203)^2}{(1.678)^2 (1.39 \times 10^{-5}) (3.8)}$$

$$R = 48$$

Dimensionless Correlation

$$\text{Sh} = -75 + 1.19(\text{Re})^{0.5} (\text{Sc})^{0.4} \quad (34)$$

$$\text{Sh} = 71.1$$

$$\text{Re} = 82.4$$

$$\text{Sc} = 666$$

$$\text{Sh} = -75 + 1.19(122) = 70$$

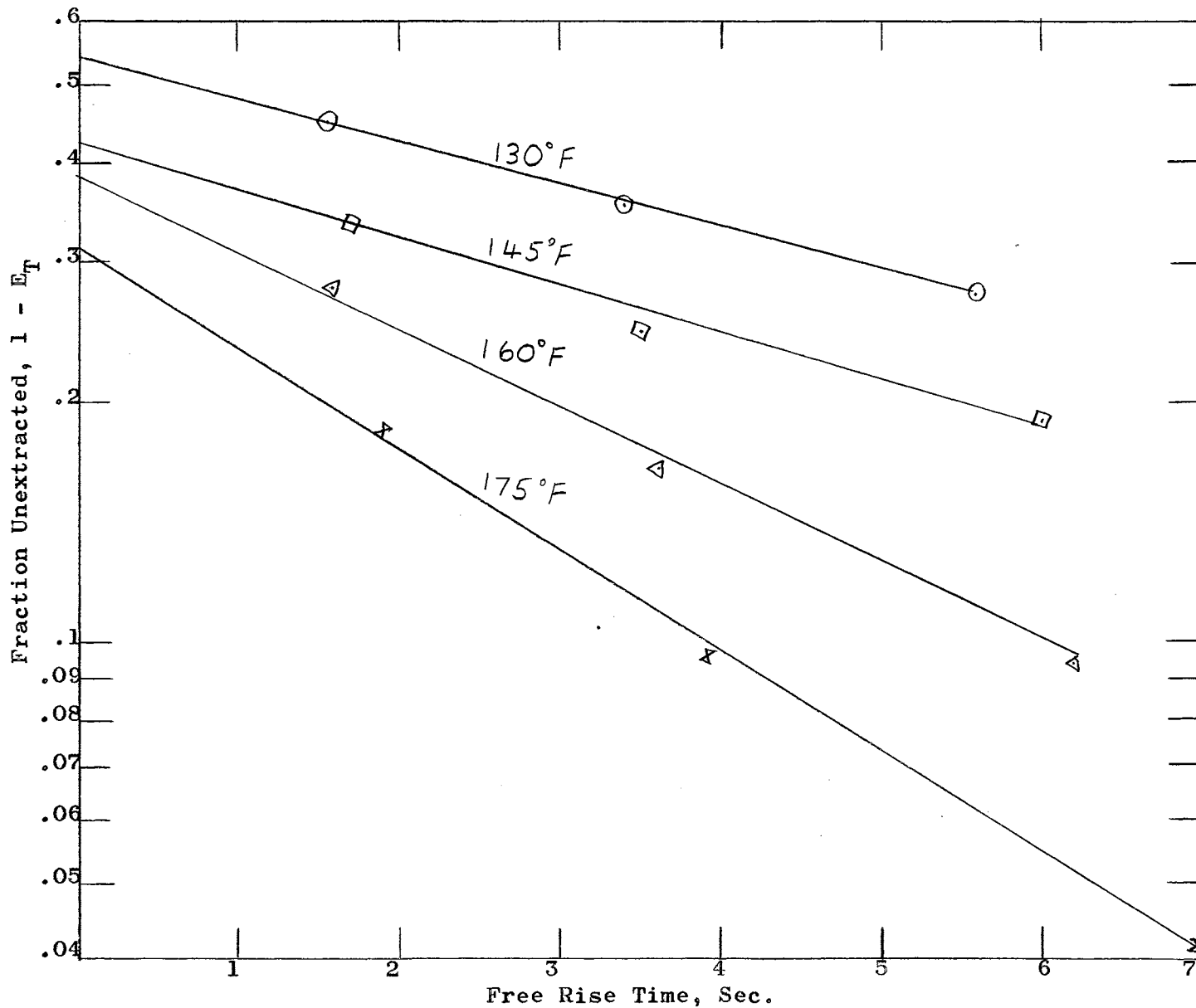


Figure 24, Effect of Free Rise Time on Transfer Efficiency Phenol + Xylene--
Cetane

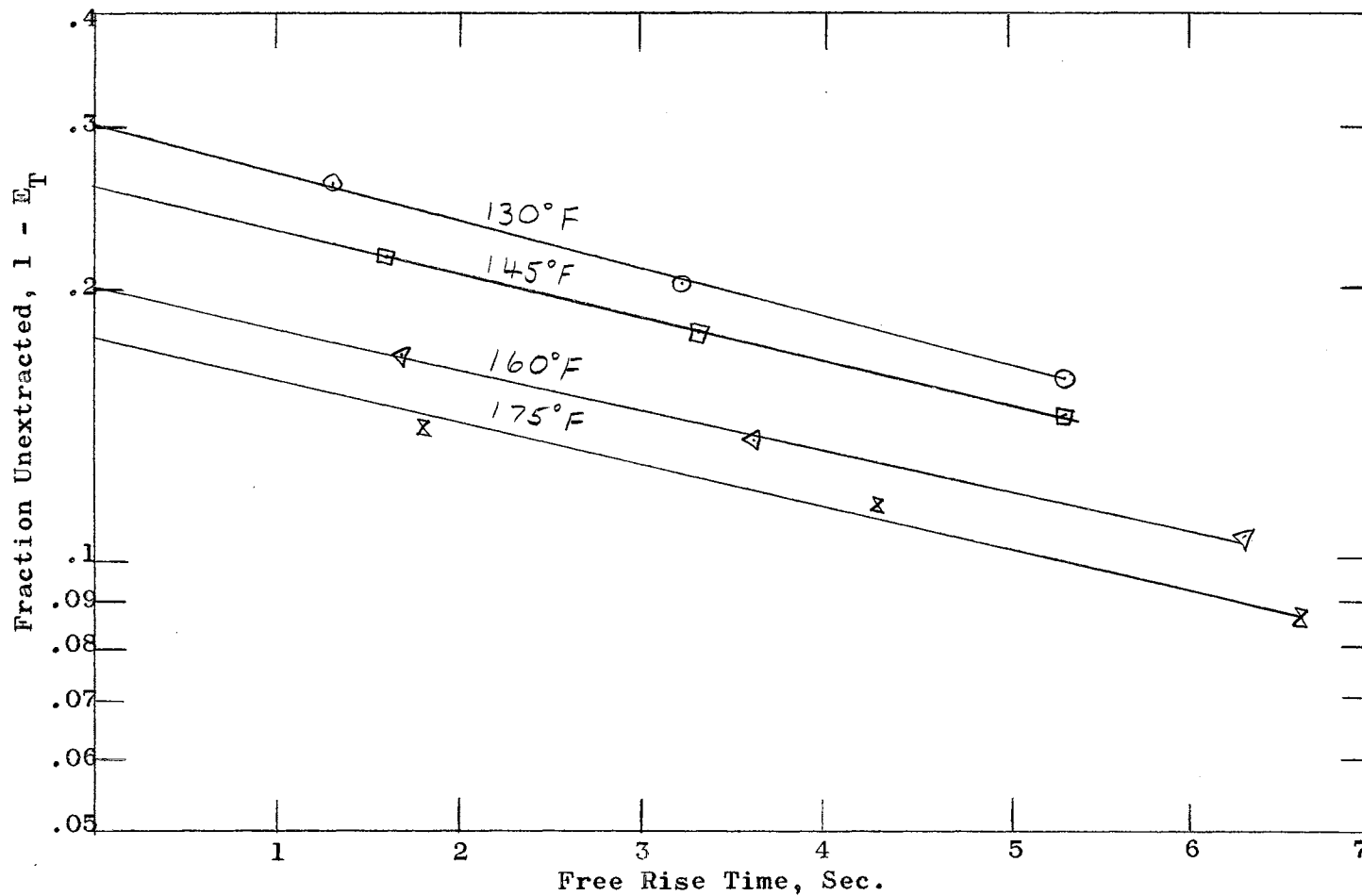


Figure 25, Effect of Free Rise Time on Transfer Efficiency for the Phenol--
Cetane + Xylene System

TABLE XII

TRANSFER OF PHENOL TO CETANE DROPS

Continuous phase = 95% aq. phenol

Dispersed phase = pure cetane

Run No.	Column height, inch	Free-rise time, sec.	Dispersed phase outlet conc., gm/gm
Temp. 130°F			
1	4	1.2	0.0463
2	8	2.5	0.049
3	12	3.8	0.0492
Temp. 145°F			
4	4	1.4	0.065
5	8	2.5	0.0685
6	12	4.0	0.0708
Temp. 160°F			
7	4	1.4	0.0755
8	8	2.6	0.0786
9	12	4.2	0.0797
Temp. 175°F			
10	4	1.6	0.0894
11	8	2.9	0.091
12	12	4.6	0.0935

The drop rate was 100/min. for all runs, and the continuous phase flow rate was 5 ml/min. for all runs.

TABLE XIII

TRANSFER OF O-XYLENE TO CETANE DROPS

Continuous phase = Phenol saturated with cetane with 11.4% xylene

Dispersed phase = Cetane saturated with phenol

Run No.	Column height, inch	Free-rise time, sec.	Dispersed phase outlet conc., gm/gm
Temp. 130°F			
13	4	1.3	0.096
14	8	3.2	0.108
15	12	5.3	0.114
Temp. 145°F			
16	4	1.6	0.111
17	8	3.3	0.116
18	12	5.3	0.120
Temp. 160°F			
19	4	1.7	0.118
20	8	3.5	0.126
21	12	5.8	0.130
Temp. 175°F			
22	4	1.8	0.112
23	8	4.3	0.115
24	12	6.6	0.120

The drop rate was 100/min. for all runs, and the continuous phase flow rate was 5 ml/min. for all runs.

TABLE XIV
TRANSFER OF O-XYLENE FROM CETANE DROPS

Continuous phase = Phenol saturated with cetane

Dispersed phase = 80.5% cetane, 19.5% o-xylene saturated with phenol

Run No.	Column height, inch	Free-rise time, sec.	Dispersed phase outlet conc., gm/gm
Temp. 130°F			
25	4	1.6	0.082
26	8	3.4	0.060
27	12	5.8	0.047
Temp. 145°F			
28	4	1.7	0.054
29	8	3.5	0.039
30	12	6.0	0.030
Temp. 160°F			
31	4	1.6	0.045
32	8	3.6	0.024
33	12	6.2	0.008
Temp. 175°F			
34	4	1.9	0.027
35	8	3.9	0.014
36	12	7.0	0.006

The drop rate was 100/min. for all runs, and the continuous phase flow rate was 5 ml/min. for all runs.

TABLE XV

CALCULATED CONCENTRATIONS OF EACH STAGE OF EXTRACTION

Temp. °F	C ₁	C ₂	C ₄	C*	K _o , cm/sec.
I. Phenol--Cetane					
130	0.000	0.0444	0.0492	0.0566	0.00496
145	0.00	0.0632	0.0708	0.0791	0.00563
160	0.00	0.0721	0.0797	0.087	0.00622
175	0.00	0.0835	0.0935	0.097	0.0056
II. Phenol saturated with cetane with 11.4% xylene--Cetane saturated with phenol					
130	0.00	0.0944	0.114	0.135	0.0042
145	0.00	0.1038	0.120	0.140	0.00464
160	0.00	0.1137	0.130	0.142	0.00412
175	0.00	0.1071	0.120	0.130	0.00334
III. Phenol saturated with cetane--80.5% cetane, 19.5% xylene saturated with phenol					
130	0.170	0.1038	0.047	0.00	0.0046
145	0.158	0.068	0.030	0.00	0.00457
160	0.155	0.0599	0.008	0.00	0.00507
175	0.147	0.042	0.006	0.00	0.0051

TABLE XVI
CALCULATED DIMENSIONLESS GROUPS

Temp.	Re	Sc	Sh	We
I. Phenol--Cetane				
130	71.25	868.0	72.3	4.86
145	82.4	666.0	71.1	5.58
160	101.1	477.0	66.0	5.8
175	101.2	375	52.2	6.14
II. Phenol saturated with cetane with 11.4% xylene--Cetane saturated with phenol				
130	61	1020	72.3	3.77
145	72.4	752	67.5	4.23
160	76.7	550	51.3	4.37
175	78.4	330	32.0	4.54
III. Phenol saturated with cetane--80.5% cetane, 19.5% xylene saturated with phenol				
130	50.0	601	60.0	3.30
145	58.0	463	52.0	3.6
160	65.8	356	49.0	4.98
175	67.7	284	44.0	7.34

TABLE XVII
CALCULATED DIMENSIONLESS GROUPS FOR USE IN
LILEEVA AND SMIRNOV'S CORRELATION

Temp.	Ki	Ar	Fo	Pr _c
I. Phenol--Cetane				
130	297	4,420	0.000314	6750
145	267	6,600	0.000417	4420
160	223	10,910	0.00058	2600
175	177	13,200	0.000718	2080
II. Phenol saturated with cetane with 11.4% xylene-Cetane saturated with phenol				
130	104	5,680	0.00106	2350
145	93.1	8,080	0.00131	1590
160	69	10,820	0.00171	1165
175	47	14,610	0.00204	830
III. Phenol saturated with cetane--80.5% cetane, 19.5% xylene saturated with phenol				
130	129	4,570	0.00102	2930
145	104	6,550	0.00131	2000
160	94.5	9,070	0.00165	1387
175	78	12,280	0.00222	1010

VITA

Charles Kennady Huff

Candidate for the Degree of

Master of Science

Thesis: LIQUID-LIQUID EXTRACTION FROM SINGLE DROPS AT
ELEVATED TEMPERATURES

Major Field: Chemical Engineering

Biographical:

Personal Data: Born in Wichita Falls, Texas, May 11,
1938, the son of William Kennady and Virginia Huff.

Education: Attended grade and high schools in Wichita
Falls, Texas; graduated from Wichita Falls Senior
High School in May, 1956; attended Baylor University
from 1956 to 1958; attended Texas Technological
College from 1958 to 1961; received the degree of
Bachelor of Science in Chemical Engineering from
Texas Technological College in August, 1961; graduate
September, 1961; completed the requirements for the
Master of Science degree in May, 1963.

Professional Societies: Associate Member of the American
Institute of Chemical Engineers.